pH-Dependent Rectification in Redox Polymers: Characterization of Electrode-Confined Siloxane Polymers Containing Naphthoquinone and Benzylviologen Subunits

G. Tayhas R. Palmore,† Diane K. Smith,‡ and Mark S. Wrighton*

Department of Chemistry, Massachusetts Institute of Technology, Cambridge, Massachusetts 02139

Received: August 25, 1996[⊗]

This paper describes the electrochemical characterization of electrode-confined siloxane polymers that contain both naphthoquinone (NQ) and benzylviologen (BV^{2+}) subunits. These "homopolymers," abbreviated (NQ-BV^{3+})$_n$ and (NQ-BV-BV^{5+})$_n$, are derived from monomers, 2-chloro-3-[[2-{dimethyl[[[[*N*′-[[4-(trimethoxysilyl)-phenyl]methyl]-4,4′-bipyridiniumyl]methyl]phenyl]methyl]ammonium}ethyl]amino]-1,4-naphthoquinone, **1a**, and 2-chloro-3-[[2-{dimethyl[[[[[[[[*N*′-[*N*′-[[4-(trimethoxysilyl)phenyl]methyl]-4,4′-bipyridiniumyl]methyl]-phenyl]methyl]-4,4′-bipyridiniumyl]methyl]phenyl]methyl]ammonium}ethyl]amino]-1,4-naphthoquinone, **2a**, respectively. Particular to these types of surface-confined homopolymers is the ability to "trap" charge at low pH in the form of reduced quinone. Between pH 10.0 and 7.0, (NQ-BV^{3+})$_n$ and (NQ-BV-BV^{5+})$_n$ undergo reversible 3e−/2H^+ and 4e−/2H^+ reduction, respectively, consistent with 2e−/2H^+ reduction of NQ subunits to the hydroquinone NQH_2 and 1e− reduction of BV^{2+} subunits to the radical cation $BV^{+\bullet}$. Below pH 6, however, NQ/NQH_2 reduction becomes irreversible in both polymers, whereas $BV^{2+/+}$ reduction remains reversible. Electrochemical irreversibility of NQ/NQH_2 in these polymers occurs because its electrochemistry is mediated by the $BV^{2+/+}$ couple. Between pH 10.0 and 7.0, $BV^{2+/+}$ can mediate both reduction and oxidation of NQ/NQH_2, whereas below pH 6, the thermodynamics are such that $BV^{2+/+}$ can only mediate the reduction of NQ. This behavior is similar to that of a previously studied (benzylviologen)−benzoquinone−(benzylviologen) polymer, (BV-Q-BV^{6+})$_n$.[1] Charge in the form of reduced quinone is trapped in (BV-Q-BV^{6+})$_n$ at low pH because there is essentially no direct charge transport through the Q/QH_2 system. Charge is also trapped in high coverages of (NQ-BV^{3+})$_n$ and (NQ-BV-BV^{5+})$_n$, indicating no direct charge transport through the NQ/NQH_2 system. Unlike (BV-Q-BV^{6+})$_n$, however, monolayers comprised of **1a** or **2a** exhibit charge transport through the NQ/NQH_2 system. The flexibility of these monolayers apparently allows direct contact of the NQ subunit with the electrode surface. Less flexible and more robust surface-confined polymers, abbreviated (NQ-BV^{3+}/siloxane)$_n$ and (NQ-BV-BV^{5+}/siloxane)$_n$, can be prepared by copolymerization of **1a** or **2a** with 1,2-bis(trimethoxysilyl)ethane. Charge trapped in (NQH_2-BV^{3+}/siloxane)$_n$ or (NQH_2-BV-BV^{5+}/siloxane)$_n$ can be released and delivered to the surface of the electrode via chemical mediation or by an increase in solution pH. For example, the redox couple I_3^-/I^- will catalytically release the trapped charge when the potential of the electrode is brought close to $E^{\circ\prime}(I_3^-/I^-)$. Surfaces modified with (NQ-BV^{3+}/siloxane)$_n$ or (NQ-BV-BV^{5+}/siloxane)$_n$, however, are impermeable to the large anionic redox couple $Fe(CN)_6^{3-/4-}$, preventing mediated charge release by this reagent. The lack of electrostatic binding of $Fe(CN)_6^{3-/4-}$ to electrodes modified with (NQ-BV^{3+}/siloxane)$_n$ or (NQ-BV-BV^{5+}/siloxane)$_n$ suggests a high degree of cross-linking in these polymers provided by 1,2-bis(trimethoxysilyl)ethane. At neutral pH, dioxygen will chemically induce the release of charge trapped in (NQH_2-BV^{3+}/siloxane)$_n$ or (NQH_2-BV-BV^{5+}/siloxane)$_n$. The irreversible production of H_2O_2 upon oxidation of NQH_2 in water, however, prevents the return of charge to the electrode. Charge release is also demonstrated by pH jump experiments where an increase in pH shifts $E^{\circ\prime}$(NQ/NQH_2) to a potential where $BV^{2+/+}$ can mediate the oxidation of NQH_2 to NQ and deliver charge to the electrode.

Introduction

In this article we describe the results of electrochemical studies of the naphthoquinone and benzylviologen containing "homopolymers," (NQ-BV^{3+})$_n$ and (NQ-BV-BV^{5+})$_n$, derived from monomers **1a** and **2a**, respectively. Results have already been reported for (BV-Q-BV^{6+})$_n$ derived from **3** that show interesting pH-dependent charge-trapping phenomena.[1−6] Electrode-confined material from **3** possesses the ability to trap charge at low pH because the electrochemistry of the two-electron quinone couple Q/QH_2 is mediated entirely by the flanking one-electron viologen couple $BV^{2+/+}$ in the same manner as bilayer assemblies of thin films.[7−14] At basic and neutral pH, the viologen mediates both reduction and oxidation of the quinone, but at acidic pH, $E^{\circ\prime}(BV^{2+/+})$ and $E^{\circ\prime}(Q/QH_2)$ are sufficiently different so as to provide a thermodynamic barrier to mediation of the oxidation of QH_2 by the $BV^{2+/+}$ subunit (Scheme 1).[1−6] Consequently, at low pH the quinone remains reduced even when the electrode is held substantially positive of the formal potential of the Q/QH_2 couple. The inability to electrochemically reoxidize the QH_2 subunit at high overpotentials illustrates the slow kinetics of electron self-exchange present in unmediated quinone electrochemistry.[10]

Our study of (NQ-BV^{3+})$_n$ and (NQ-BV-BV^{5+})$_n$ was undertaken to assess the generality of pH-dependent rectification in quinone-viologen polymers. The redox potential of naphthoquinone in (NQ-BV^{3+})$_n$ and (NQ-BV-BV^{5+})$_n$ is similar to that

* Address correspondence to this author at Washington University, St. Louis, MO 63130.

† Present address: Department of Chemistry, University of California, Davis, CA 95616.

‡ Present address: Department of Chemistry, San Diego State University, San Diego, CA 92109.

⊗ Abstract published in *Advance ACS Abstracts,* March 1, 1997.

S1089-5647(96)02647-8 CCC: $14.00

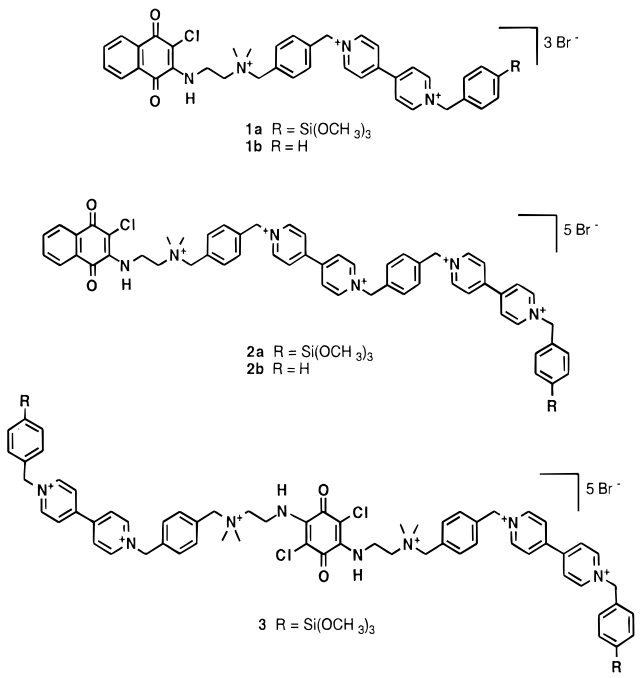

of benzoquinone in **3**. The noteworthy differences between $(NQ\text{-}BV^{3+})_n$, $(NQ\text{-}BV\text{-}BV^{5+})_n$, and $(BV\text{-}Q\text{-}BV^{6+})_n$ are the ratio of viologen to quinone per monomer unit (1:1 for **1a**, 2:1 for **2a** and **3**), the number of trimethoxysilyl groups per monomer unit (1 for **1a** and **2a**, 2 for **3**), and the structural relationship between viologen and quinone in the different monomers. Any of these differences could affect the ability of these polymers to trap charge by altering the rate of electron self-exchange between quinone centers. For both $(NQ\text{-}BV^{3+})_n$ and $(NQ\text{-}BV\text{-}BV^{5+})_n$, polymeric coverages ($>1 \times 10^{-9}$ mol cm^{-2}) show pH-dependent charge trapping. Unlike $(BV\text{-}Q\text{-}BV^{6+})_n$, however, some direct charge transport to the quinone subunits is observed in monolayers of **1a** and **2a**, precluding molecular rectification at monolayer coverages.

A consequence of the single trimethoxysilyl group per monomer of **1a** and **2a** is that both monolayer and polymeric coverages of $(NQ\text{-}BV^{3+})_n$ or $(NQ\text{-}BV\text{-}BV^{5+})_n$ are typically less durable than corresponding coverages of $(BV\text{-}Q\text{-}BV^{6+})_n$. More durable polymers, abbreviated $(NQ\text{-}BV^{3+}/\text{siloxane})_n$ and $(NQ\text{-}BV\text{-}BV^{5+}/\text{siloxane})_n$, can be prepared by copolymerizing **1a** or **2a**, respectively, with the siloxane reagent 1,2-bis(trimethoxysilyl)ethane. Electrodes modified with $(NQ\text{-}BV^{3+}/\text{siloxane})_n$ or $(NQ\text{-}BV\text{-}BV^{5+}/\text{siloxane})_n$ behave similarly to those modified with $(NQ\text{-}BV^{3+})_n$ and $(NQ\text{-}BV\text{-}BV^{5+})_n$, but are substantially more durable. Complete electrochemical reversibility is observed in $(NQ\text{-}BV^{3+}/\text{siloxane})_n$ and $(NQ\text{-}BV\text{-}BV^{5+}/\text{siloxane})_n$ at pH's above 6.0. Below pH 6.0, the $1ne^-$'s associated with the $BV^{+\bullet}$ subunits are reversibly removed from the polymers, whereas the $2ne^-$'s associated with NQH_2 remain largely inaccessible or "trapped". For pH < 3.0, potentials up to 1.0 V positive of $E^{o\prime}(NQ/NQH_2)$ do not reoxidize the NQH_2 subunits. Methods to chemically induce the release of charge trapped in $(NQH_2\text{-}BV^{3+}/\text{siloxane})_n$ and $(NQH_2\text{-}BV\text{-}BV^{5+}/\text{siloxane})_n$ are described.

Experimental Section

Chemicals and General Equipment. Tetrahydrofuran (THF) was distilled prior to use from sodium benzophenone ketyl. Dimethyl sulfoxide (DMSO) was distilled from BaO under vacuum and stored over 3 Å molecular sieves. CH_3CN was distilled from CaH_2 followed by distillation from P_2O_5 and stored over 3 Å molecular sieves. All other chemicals, including electrolytes and buffer materials, were reagent grade and used as received from commercial sources. ^{1}H NMR spectra (referenced to tetramethylsilane) were recorded on a Bruker WM-250 MHz, a Varian XL-300 MHz, or a Varian VXR-500 MHz spectrometer as indicated. UV−vis spectra were recorded on a Hewlett-Packard 8451A rapid-scan or Vectra ES/12 spectrophotometer. Melting points were determined with a Hoover capillary melting point apparatus and are uncorrected. Mass spectral data were collected on a Finnigan MAT-8200 mass spectrometer. X-ray photoelectron spectra were obtained using a Surface Science Laboratories SSX-100 spectrometer with signals referenced to C(1s) at 284.6 eV. Elemental analyses were performed by Oneida Research Services, Inc., or Galbraith Laboratories.

SCHEME 1: pH-Dependent Electrochemical Behavior of Quinone−Viologen Polymer

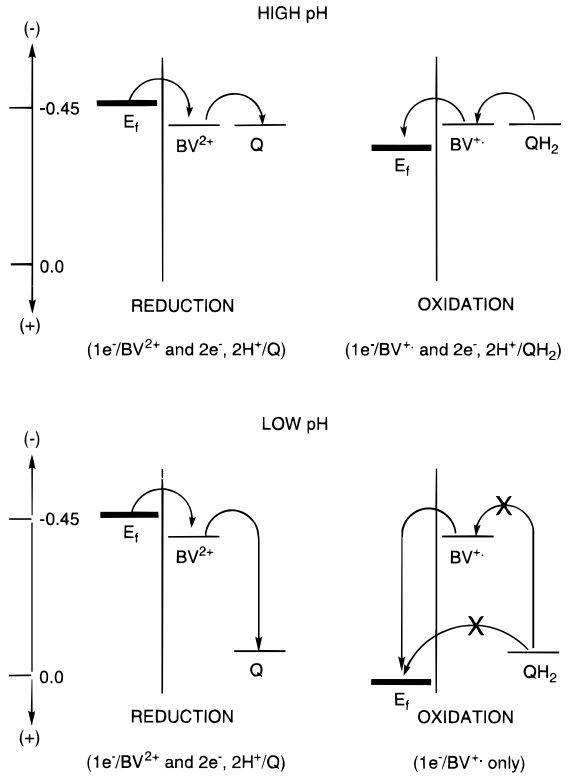

Electrochemical Equipment and Procedures. Electrochemical experiments were performed using either a PAR Model 363 potentiostat/galvanostat and a PAR Model 175 universal programmer or a Pine Model RDE4 bipotentiostat. Current−voltage responses were recorded with a Kipp and Zonen BD91 $x-y-y'$ recorder. All electrochemical experiments were carried out under argon in a one-compartment cell using a standard three-electrode configuration with a Pt counter electrode and a saturated calomel (SCE) reference electrode. Electrolyte solutions were prepared using glass-distilled H_2O. pH 10 through 7.4 electrolyte solutions were buffered with 0.1 M tris(hydroxymethyl)aminomethane (Tris) and adjusted to the desired pH with HCl. pH 6 through 4 electrolyte solutions were buffered with 0.1 M sodium acetate and adjusted to the desired pH with acetic acid. pH 3 electrolyte solution was 0.1 M potassium hydrogen phthalate and adjusted to pH 3 with HCl. pH 1.1 electrolyte solution was adjusted with H_2SO_4. Electrolyte concentrations for pH 10.0 to 4.0 were 1.0 M LiCl.

Electrodes and Electrode Derivatization. Kel-F-sealed glassy carbon electrodes (Bioanalytical Systems, 0.071 cm^2) and white epoxy-sealed indium-doped SnO_2 (ITO) electrodes (fab-

ricated from indium-doped SnO_2-coated glass obtained from Delta Technologies) were used for the modified electrode experiments. The carbon electrodes were polished prior to derivatization first with 1 μm of a-Al_2O_3, followed with 0.05 μm of g-Al_2O_3 (Micropolish II, Buehler). The ITO electrodes were cleaned prior to derivatization by sonication in soapy H_2O for 15 min, followed by sonication in clean H_2O for 15 min. Both the glassy carbon and ITO electrodes were further pretreated by soaking in 1 M NaOH for 10 min prior to derivatization. Epoxy-sealed Au flag electrodes were used for solution electrochemistry and were cleaned prior to use by cycling in 1 M H_2SO_4 between +1.2 and −0.4 V vs SCE at 100 mV/s for 15−30 min.

Electrodes were derivatized with (NQ-BV^{3+})$_n$ or (NQ-BV-BV^{5+})$_n$ by soaking or potentiostatting (−0.7 V vs SCE) the electrodes in a 1 mM solution of the monomers dissolved in 0.2 M KCl/0.1 M K_2HPO_4 electrolyte. Depending on the length of time the electrode was held in the derivatizing solution, the coverage of polymer was typically between 1×10^{-10} and 3×10^{-9} mol cm^{-2}. Larger coverages were obtained by stirring during derivatization. The electrodes were subsequently soaked in pH 7.4 Tris buffer/1.0 M KCl for at least 15 h.

Electrodes modified with (NQ-BV^{3+}/siloxane)$_n$ or (NQ-BV-BV^{5+}/siloxane)$_n$ were prepared by the addition of an equimolar amount of 1,2-bis(trimethoxysilyl)ethane (Petrarch) to derivatizing solutions containing 1 mM **1a** or **2a** in aqueous 0.2 M KCl/0.1 M K_2HPO_4. This mixture was left to hydrolyze for ∼5 min while being purged with argon. Electrodes were then immersed in the derivatizing solution, placed under potential control, and cycled between −0.2 and −0.6 V vs SCE at 10 mV/s while the solution was stirred. Typically, several electrodes were derivatized in the same derivatizing solution and subsequently soaked in pH 7.4 Tris buffer/1.0 M KCl for at least 15 h. Depending on the length of time the electrode was held in the derivatizing solution, coverages of $\sim 5 \times 10^{-9}$ mol cm^{-2} were produced.

pH Jump Experiments. Experiments to demonstrate the release of charge trapped in (NQH_2-BV^{3+}/siloxane)$_n$ or (NQH_2-BV-BV^{5+}/siloxane)$_n$ via an abrupt change in solution pH were performed as follows: in a single-compartment electrochemical cell containing 10 mL of electrolyte (0.5 M KCl/pH 3.0 phosphate buffer, purged with argon), a glassy carbon rotating disc electrode (RDE) modified with either (NQ-BV^{3+}/siloxane)$_n$ or (NQ-BV-BV^{5+}/siloxane)$_n$ was rotated at 200 rpm. The current vs time response was monitored as the electrode potential was stepped from +0.2 to −0.6 V and back to +0.2 V vs SCE. Upon addition of ∼0.5 mL of deoxygenated 1 M NaOH, the solution pH increased to >9.0, with the corresponding release of trapped charge seen as a transient anodic current in the current−time profile.

Synthesis of 4,[15−17] **7a**[2](*N*-[[4-(trimethoxysilyl)phenyl]-methyl]-4,4′-bipyridinium), and **7b**[15−17] (*N*-(phenylmethyl)-4,4′-bipyridinium) was performed using previously reported procedures.

Synthesis of 5a. Under an inert atmosphere, 0.4 g (1.5 mmol) of **4** and 2.8 g (11.3 mmol) of *p*-(trimethoxysilyl)benzyl chloride were added to 15 mL of anhydrous CH_3CN. The solution was stirred at reflux for 2 h. The precipitate was filtered and washed with 100 mL of anhydrous THF to give 0.7 g (73%) of pure product. ^{1}H NMR (300 MHz, DMSO-d_6): δ 8.09 (d, 2H), 7.95−7.75 (dt, 2H), 7.8−7.6 (dd, 4H), 4.7 (s, 2H), 4.3 (m, 2H), 3.7 (t, 2H), 3.6 (s, 9H), 3.1 (s, 6H).

Synthesis of 5b. 2-Chloro-3-[[2-[dimethyl(phenylmethyl)-ammonium]ethyl]amino]-1,4-naphthoquinone was prepared by combining 0.4 g (1.4 mmol) of **4** with 1 mL of benzyl bromide in 10 mL of acetone and stirring at room temperature for 2 h. The orange precipitate was filtered, washed with acetone, and dried under vacuum to give 0.6 g (98%) of pure product, mp = 203 °C. ^{1}H NMR (250 MHz, DMSO-d_6): δ 8.03 (m, 2H), 7.82 (dtd, 2H), 7.55 (m, 5H), 4.63 (s, 2H), 4.23 (t, 2H), 3.62 (t, 2H), 3.05 (s, 6H). UV−vis is (H_2O): ϵ = 18 350 M^{-1} cm^{-1} at λ_{272} and 3,350 M^{-1} cm^{-1} at λ_{460}.

Synthesis of 5c. To a 500 mL flask containing dry CH_2Cl_2 (400 mL) were added 5.0 g (17.9 mmol) of **4** and 9.5 g (35.8 mmol) of α,α′-dibromo-*p*-xylene. After being stirred at reflux overnight, the orange precipitate was filtered and washed with copious amounts of CH_2Cl_2 and THF to give 8.9 g (92%) of pure product, mp = 191 °C. ^{1}H NMR (300 MHz, CD_3OD): δ 8.07 (dm, 2H), 7.77 (dtd, 2H), 7.60 (s, 4H), 4.64 (s, 2H), 4.62 (s, 2H), 4.31 (t, 2H), 3.68 (t, 2H), 3.16 (s, 6H). ^{1}H NMR (250 MHz, DMSO-d_6): δ 7.99 (d, 2H), 7.81 (m, 2H), 7.58 (m, 4H), 4.77 (s, 2H), 4.61 (s, 2H), 4.21 (d, 2H), 3.58 (t, 2H), 3.04 (s, 6H). HRMS: *m/z* 461.0628 ([M − Br]$^+$), calcd for $C_{22}H_{23}BrClN_2O_2$, 461.06314. Anal. Calcd for $C_{22}H_{23}Br_2ClN_2O_2$: C, 48.68; H, 4.24; N, 5.16; Cl, 6.55. Found: C, 48.38; H, 4.23; N, 5.14; Cl, 6.95.

Synthesis of 6. **5c** (1.8 g, 3.1 mmol) and 6.1 g (39.2 mmol) of 4,4′-bipyridine were refluxed in 200 mL of dry CH_3CN overnight. The yellow-orange solid was collected by filtration and purified on a column packed with neutral alumina (2.5 cm diameter × 12 cm length). The excess 4,4′-bipyridine was separated from the product with 100% CH_3CN as eluent. The product was then removed from the column with 100% CH_3OH as eluent. Removal of solvent gave a red oil that was recrystallized from CH_3OH to give red crystals (1.8 g, 77%), mp = 182−183 °C. ^{1}H NMR (250 MHz): (DMSO-d_6) δ 9.39 (d, 2H), 8.87 (d, 2H), 8.67 (d, 2H), 8.03 (d, 2H), 7.98 (d, 2H), [7.81 (m, 2H), 7.70 (m, 4H), overlapping peaks], 5.97 (s, 2H), 4.65 (s, 2H), 4.21 (d, 2H), 3.61 (t, 2H), 3.04 (s, 6H); CD_3OD) δ 9.01 (d, 2H), 8.74 (d, 2H), 8.31 (d, 2H), 8.03 (d, 2H), 7.98 (dd, 2H), [7.72 (s, 4H) and 7.74 (m, 2H), overlapping peaks], 5.99 (s, 2H), 4.72 (s, 2H), 4.30 (t, 2H), 3.69 (t, 2H), 3.20 (s, 6H); (CD_3CN) δ 8.86 (dd, 4H), 8.35 (d, 2H), 8.04 (dd, 2H), 7.93 (d, 2H), 7.76 (dt, 2H), 7.62 (m, 4H). HRMS: *m/z* 617.1313 ([M − Br]$^+$), calcd for $C_{32}H_{31}BrClN_4O_2$, 617.13188.

Synthesis of 1a. Under an inert atmosphere, 82 mg (0.12 mmol) of **6** and 450 mg (1.8 mmol) of *p*-(trimethoxysilyl)benzyl chloride were added to 5 mL of anhydrous DMSO. The orange solution was left stirring at 70 °C for 4 h followed by the addition of 250 mL of anhydrous THF to precipitate an orange solid. The solid was filtered and dried under vacuum to give **1a** (125 mg, >95%). ^{1}H NMR (300 MHz, DMSO-d_6): δ 9.75 (d, 2H), 9.65 (d, 2H), 8.85 (d, 4H), 8.00 (d, 2H), 7.9−7.6 (m, 10H), 6.15 (s, 2H), 6.05 (s, 2H), 4.75 (s, 2H), 4.25 (bm, 2H), 3.60 (t, 2H), 3.50 (s, 9H), 3.15 (s, 6H).

Synthesis of 1b. Benzyl bromide was used instead of *p*-(trimethoxysilyl)benzyl chloride to prepare **1b**. ^{1}H NMR (300 MHz, CD_3CN, PF_6^- salt): δ 8.95 (dd, 4H), 8.39 (dd, 4H), 8.03 (d, 2H), 7.75 (dt, 2H), 7.61 (s, 4H), 7.51 (s, 5H), 6.51 (bm, 1H), 5.87 (s, 2H), 5.82 (s, 2H), 4.22 (q, 2H), 3.99 (s, 2H), 3.54 (t, 2H), 3.02 (s, 6H). ^{1}H NMR (250 MHz, DMSO-d_6): δ 9.58 (dd, 4H), 8.80 (dd, 4H), 7.99 (d, 2H), 7.90−7.39 (m, 11H), 6.07 (s, 2H), 5.99 (s, 2H), 4.69 (s, 2H), 4.22 (q, 2H), 3.62 (t, 2H), 3.09 (s, 6H). UV−vis (H_2O): ϵ = 41 000 M^{-1} cm^{-1} at λ_{267} and 3300 M^{-1} cm^{-1} at λ_{460}. HRMS: *m/z* 708.1869 ([M − 2Br]$^+$), calcd for $C_{39}H_{38}ClN_4O_2Br$, 708.1866631. Anal. Calcd for $C_{39}H_{38}ClBr_3N_4O_2 \cdot 3H_2O$: C, 50.69; H, 4.77; N, 6.07. Found: C, 51.12; H, 4.78; N, 5.95.

Synthesis of 8a. Under an inert atmosphere, 1.1 g (4.1 mmol) of α,α′-dibromo-*p*-xylene and 0.5 g (1.1 mmol) of **7a** were

SCHEME 2

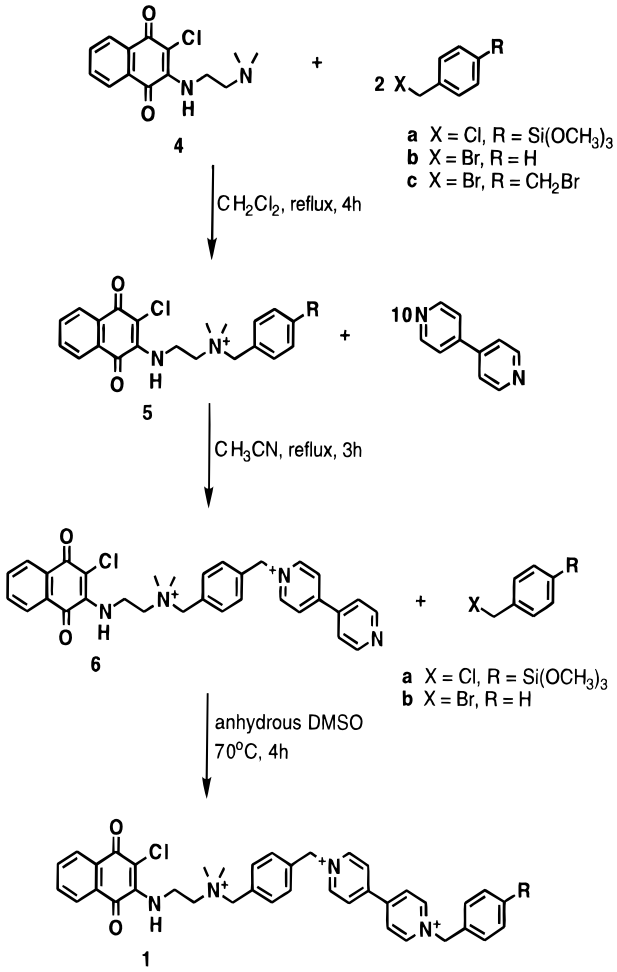

dissolved in 20 mL of anhydrous CH_3CN. The reaction mixture was refluxed under argon overnight, followed by the addition of 250 mL of anhydrous THF. The resultant slurry was stirred for 20 min, filtered, and washed with 100 mL of anhydrous THF to yield **8a** (0.8 g, >95%) as a bright yellow solid. ^{1}H NMR (250 MHz, DMSO-d_6): δ 9.55 (d, 2H), 8.75 (d, 2H), 7.69−7.45 (m, 8H), 6.00 (s, 2H), 5.95 (s, 2H), 4.72 (s, 2H), 3.53 (s, 9H).

Synthesis of 8b. The procedure used for the preparation of **8a** was used for the preparation of **8b**, substituting **7b** in place of **7a**. ^{1}H NMR (250 MHz): (DMSO-d_6) δ 9.52 (d, 4H), 8.73 (d, 4H), 7.65−7.41 (m, 9H), 5.93 (s, 4H), 4.69 (s, 2H); (D_2O) δ 9.00 (d, 4H), 8.38 (d, 4H), 7.48−7.32 (m, 9H), 5.78 (s, 4H), 4.45 (s, 2H); (CD_3OD) δ 9.35 (d, 4H), 8.69 (d, 4H), 7.59−7.49 (m, 9H), 5.99 (s, 4H), 4.60 (s, 2H). The bromide salt was metathesized to the PF_6^- salt by dissolving **8b** in minimal H_2O, filtering any leftover solids, and adding this solution to a solution saturated with $NH_4^+PF_6^-$. The mixture was stirred for 20 min; the precipitate was filtered, washed with H_2O, and dried under vacuum to give a white powder. ^{1}H NMR (250 MHz, CD_3CN, PF_6^- salt): δ 8.97 (d, 4H), 8.37 (d, 4H), 7.60−7.45 (m, 9H), 5.82 (s, 4H), 4.60 (s, 2H).

Synthesis of 2a. Under an inert atmosphere, 105 mg (0.15 mmol) of **6** and 100 mg (0.15 mmol) of **8a** were combined in 6.0 mL of anhydrous DMSO. The orange-red reaction mixture was stirred under argon at 70 °C for 4 h. The reaction slurry was subsequently transferred to a flask containing 25 mL of anhydrous CH_3CN. The resultant slurry was stirred for 1 h, followed by vacuum filtration. The filtered solid was washed with 100 mL of anhydrous THF to give 18 mg (89%) of an

SCHEME 3

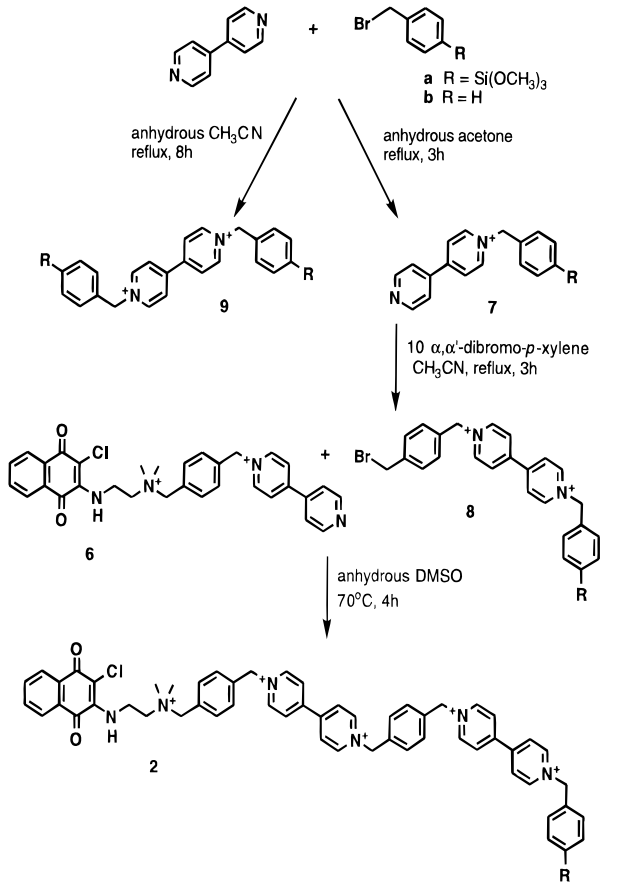

orange solid. ^{1}H NMR (300 MHz, DMSO-d_6): δ 9.61 (m, 8H), 8.82 (m, 8H), 8.00 (d, 2H), 7.92−7.45 (m, 14H), 6.75 (bm, 1H), 6.02 (m, 8H), 4.68 (m, 2H), 4.22 (m, 2H), 3.61 (m, 2H), 3.35 (obscured by NMR solvent, 9H), 3.07 (s, 6H).

Synthesis of 2b. To a 10 mL flask containing 5 mL of DMSO were added 92 mg (0.11 mmol) of **6** and 63 mg (0.11 mmol) of **8b**. The reaction mixture was stirred at 70 °C for 4 h. Reaction progress was monitored by TLC (9:0.5:0.5 CH_3CN/H_2O/saturated KNO_3). The resultant slurry was added to 100 mL of CH_3CN and filtered to give an orange precipitate. The precipitate was washed with an additional 100 mL of CH_3CN and 100 mL of diethyl ether to give 70 mg (46%) of product. ^{1}H NMR (300 MHz): (DMSO-d_6) δ 9.55 (m, 8H), 8.79 (m, 8H), 8.00 (d, 2H), 7.85−7.42 (m, 15H), 5.99 (m, 8H), 4.65 (s, 2H), 4.22 (m, 2H), 3.61 (m, 2H), 3.05 (s, 6H); (CD_3OD) δ 9.34 (m, 8H), 8.68 (m, 8H), 8.05 (d, 2H), 7.85−7.45 (m, 15H), 6.06 (s, 2H), 6.04 (s, 4H), 5.97 (s, 2H), 4.71 (s, 2H), 4.30 (t, 2H), 3.69 (t, 2H), 3.20 (s, 6H). UV−vis is (H_2O): $\epsilon = 70\,500\ M^{-1}\ cm^{-1}$ at λ_{267} and $3300\ M^{-1}\ cm^{-1}$ at λ_{460}. Anal. Calcd for $C_{57}H_{54}Br_5ClN_6O_2 \cdot 5H_2O$: C, 49.60; H, 4.64; N, 6.09. Found: C, 48.27; H, 4.59; N, 5.95.

Results and Discussion

Synthesis and Electrode Derivatization. Schemes 2 and 3 illustrate the synthetic steps used to prepare compounds **1** and **2**, respectively. Electrodes were derivatized with $(NQ\text{-}BV^{3+})_n$ using **1a** or $(NQ\text{-}BV\text{-}BV^{5+})_n$ using **2a** by procedures analogous to those used to modify electrodes with $(BV\text{-}Q\text{-}BV^{6+})_n$ or the benzyl viologen polymer **9a**.[1,15] Our procedure, which involves holding the electrode at −0.7 V vs SCE in a slightly basic solution of the monomer, takes advantage of the differing solubilities of BV^{2+} and $BV^{+\bullet}$ in aqueous solution. At −0.7 V, hydrophilic BV^{2+} subunits of **1a** or **2a** are reduced to

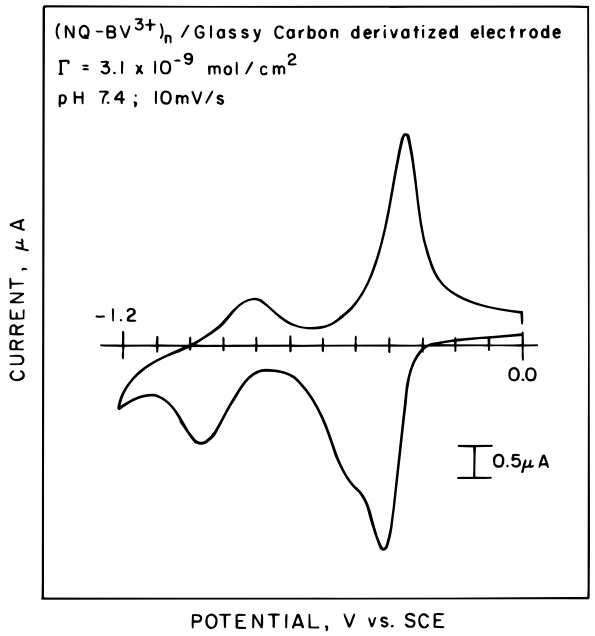

Figure 1. Cyclic voltammogram obtained in 1 M LiCl/pH 7.4 Tris buffer at 10 mV/s using a glassy carbon electrode modified with (NQ-BV^{3+})$_n$. The NQ/NQH_2 couple ($2e^-/2H^+$) appears as a reversible wave at −0.38 V. The first and second reductions ($1e^-$) of the benzylviologen subunit appear at −0.45 and −0.87 V, respectively.

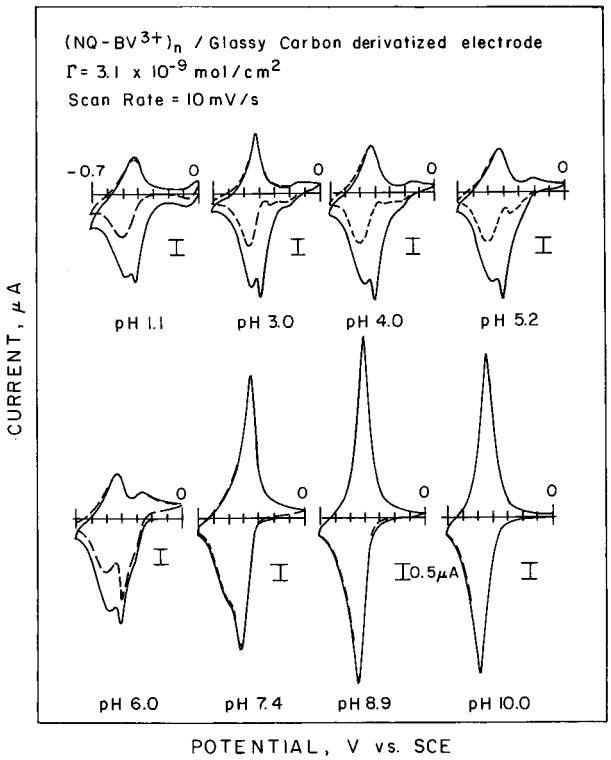

Figure 2. pH-dependent cyclic voltammograms of a glassy carbon electrode derivatized with (NQ-BV^{3+})$_n$. The potential was swept between 0.0 and −0.7 V vs SCE at 10 mV/s. The solid line is the first scan, and the dashed line is the second and all subsequent scans. The small, pH-dependent wave that appears at acidic pH represents NQ subunits directly accessible to the electrode. The difference between the integrated areas of the cathodic waves in the first and second scans represents the amount of charge trapped as NQH_2.

hydrophobic $BV^{+\bullet}$, causing the monomer to precipitate onto the electrode. The resulting high concentration of trimethoxysilyl groups leads to rapid condensation and polymerization under the basic conditions used, giving electrochemically deposited coverages of naphthoquinone−viologen polymers that can exceed 10^{-9} mol cm^{-2}. Coverage (Γ) was determined by integration of the cyclic voltammogram at neutral pH at a scan rate slow enough (10 mV/s) to accurately reflect actual coverage.

Cyclic Voltammetry of Electrode-Confined (NQ-BV^{3+})$_n$. Figure 1 shows the cyclic voltammogram of a glassy carbon electrode derivatized with (NQ-BV^{3+})$_n$. The electrochemistry of the naphthoquinone subunit, which undergoes a $2e^-/2H^+$ reduction, is observed as a large wave at −0.38 V vs SCE, near the potential where the electrochemistry of NQ/NQH_2 in **5a** or **5b** appears at the same pH. The first ($BV^{2+/+}$) and second ($BV^{+/0}$) reduction waves of the benzylviologen subunit in (NQ-BV^{3+})$_n$ occur at ∼−0.45 V (as a shoulder to the NQ/NQH_2 wave) and −0.87 V, respectively, close to where they appear in (BV-Q-BV^{6+})$_n$. The combined area of the NQ/NQH_2 and $BV^{2+/+}$ waves is approximately three times larger than the $BV^{+/0}$ wave, in accord with a $3e^-/2H^+$ reduction vs a $1e^-$ reduction, respectively.

Evidence for mediation of the redox process of NQ/NQH_2 by $BV^{2+/+}$ is illustrated in the cyclic voltammograms of (NQ-BV^{3+})$_n$ at different pHs (Figure 2). Between pH 10.0 and 7.4, reduction of both $BV^{2+/+}$ and NQ/NQH_2 centers is completely reversible. At lower pHs, however, reduction of NQ becomes irreversible, even at a slow scan rate of 10 mV/s. The second scan (dashed lines) at low pHs represents only the current for reduction and oxidation of BV^{2+}, indicating that the NQ/NQH_2 centers remain reduced.

The pH dependence of the cyclic voltammograms of equivalent coverages of (NQ-BV^{3+})$_n$ and (BV-Q-BV^{6+})$_n$ on glassy carbon electrodes appear quite similar.[1,2] A notable exception, however, is the presence of a small reversible wave in the second scan at low pH in Figure 2. This wave occurs at the expected potential of the NQ/NQH_2 couple (e.g., ∼−0.17 V vs SCE at pH 4.0) and represents only a small fraction of the NQ/NQH_2 present. The fact that most of the NQ centers are reduced on the first cycle near the onset of the $BV^{2+/+}$ wave and negative of the small reversible wave, indicates that, like reduction of Q in (BV-Q-BV^{6+})$_n$, reduction of the NQ subunit in (NQ-BV^{3+})$_n$ occurs largely via mediation by the $BV^{2+/+}$ subunit.

Monolayers of **1a** were also investigated for pH-dependent charge trapping (Figure 3). Significant differences in behavior were observed in monolayers of **1a** compared to monolayers of **3**.[1,2] At pHs where charge trapping is expected, approximately 50% of the NQ subunits in (NQ-BV^{3+})$_n$ are directly accessible to the electrode, seen as the *pH-dependent* wave (unmediated by BV^{2+}) that shifts from ∼0.15 V at pH 3.0 to ∼−0.45 V at pH 8.9 (Figure 3, part a). Charge trapping still occurs at this coverage, but to a much lesser degree compared to that for monolayers of **3**. At lower coverages of **1a** ($\Gamma = 2.4 \times 10^{-10}$ mol cm^{-2}), trapping of charge is not observed at any pH (Figure 3, part b). The difference in charge-trapping behavior of monolayers of **1a** and **3** may be due to the inherent flexibility of **1a**. Monolayers of **1a** are attached to the electrode surface by a single trimethoxysilyl moiety, as opposed to two for **3**, and therefore may be flexible enough for the NQ subunit to come into direct contact with the electrode surface.

The electrochemical behavior of an ITO electrode modified with a high coverage of (NQ-BV^{3+})$_n$ ($\Gamma = 1.5 \times 10^{-9}$ mol cm^{-2}, data not shown) at different pHs is essentially the same as that observed using a glassy carbon electrode (see Figure 2). The electrochemical behavior of an ITO electrode modified with a monolayer of **1a**, however, exhibits charge trapping at coverages where no charge trapping occurs in monolayers of **1a** on glassy carbon (compare Figure 4 with Figure 3, part b). The inability of monolayers of **1a** confined to glassy carbon to trap charge

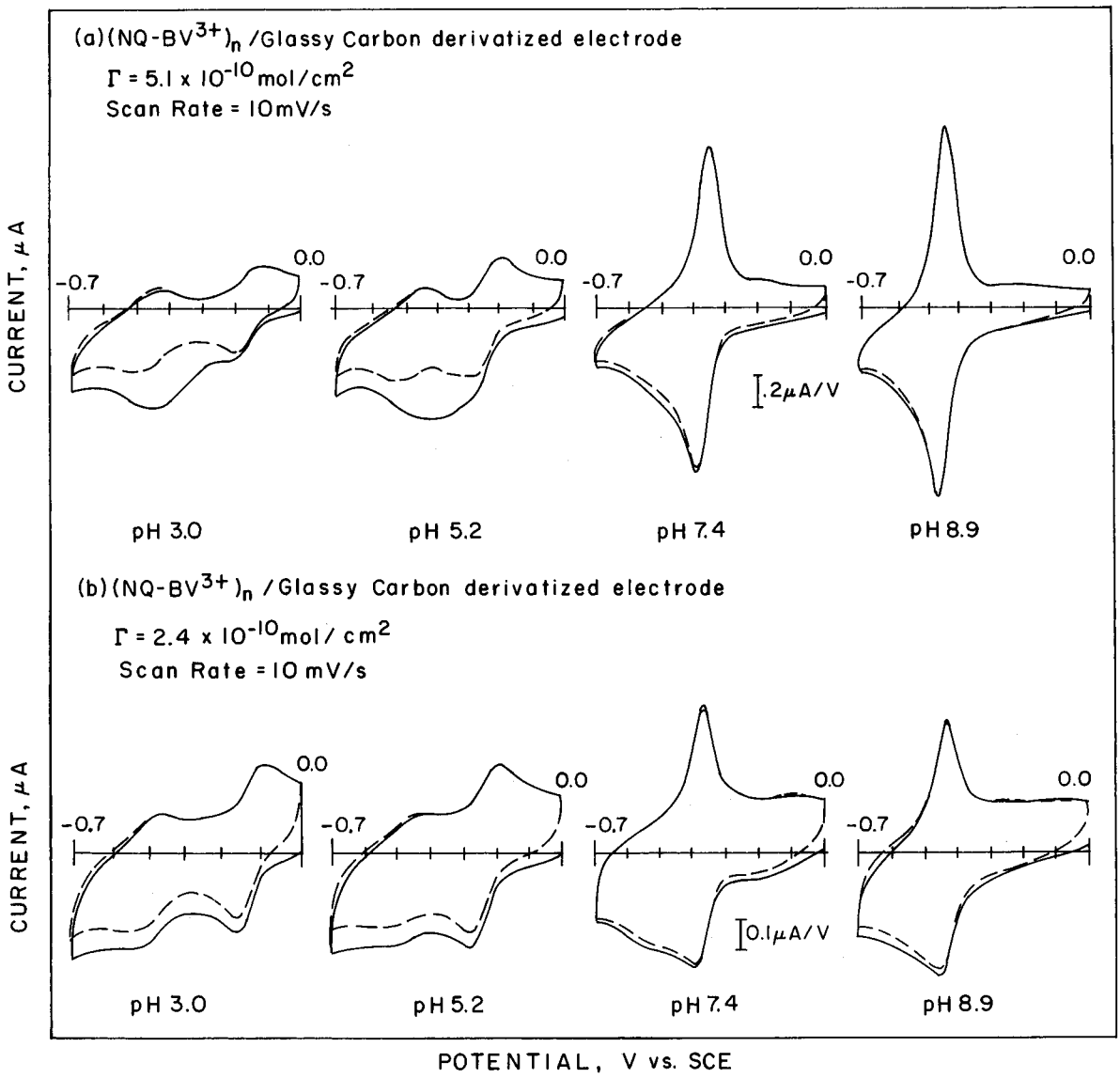

Figure 3. pH-dependent cyclic voltammograms of glassy carbon electrodes modified with a monolayer of **1a**: (a) $\Gamma = 5.1 \times 10^{-10}$ mol cm^{-2}; (b) $\Gamma = 2.4 \times 10^{-10}$ mol cm^{-2}. The experimental conditions are the same as those described for Figure 2. For the electrode used in (a), approximately 50% of the NQ subunits are directly accessible to the electrode surface [appears as the reversible, pH-dependent wave at ~ -0.25 V (pH 5.2) and ~ -0.15 V (pH 3.0)]. For the electrode used in b, essentially no trapping of charge occurs at low pH since ~90% of the NQ subunits are directly accessible to the electrode surface.

at low pH may be due to the strong adsorption properties of quinones to carbon and Pt surfaces.[18,19]

Cyclic Voltammetry of 1b. Shown in Figure 5 are the cyclic voltammograms of **1b** at pH 7 and 4 compared to those of an equimolar mixture of naphthoquinone, **5b**, and benzyl viologen, **9b**. The cyclic voltammograms obtained from a mixture of **5b** and **9b** are those expected on the basis of the cyclic voltammograms of **5b** and 9b separately determined. The cyclic voltammogram of **1b** at pH 7 is also that expected on the basis of a 1:1 mixture of quinone and viologen, the only differences being that the $BV^{2+/+}$ wave is more positive in **1b** than in **9b** and slightly distorted due to stripping of material that precipitated onto the electrode during reduction. The NQ/NQH_2 wave in both **1b** and **5b** occurs essentially at the same potential. At pH 4, however, the NQ/NQH_2 wave in **1b** is quite different from the NQ/NQH_2 wave in **5b**. The cathodic peak of NQ/NQH_2 in **1b** shifts negative to that in **5b** and the anodic wave becomes drawn out. This behavior is similar to that observed for BV-Q-BV^{6+} in acidic solution and can be explained with similar arguments:[1] a small amount of NQ-BV^{3+} persistently adsorbs to the electrode so reduction and oxidation of the solution species is actually mediated by a layer of surface-adsorbed NQ-$BV^{2+\bullet}$. As in the polymer, oxidation of NQH_2 in **1b** is slow at acidic pH because the $BV^{2+/+}$ is unable to mediate the oxidation of NQH_2 and because of the slow rate of electron self-exchange between NQ/NQH_2 subunits. The difference between the electrochemical behavior of NQ-BV^{3+} and BV-Q-BV^{6+} in solution, like the difference between surface-confined $(NQ\text{-}BV^{3+})_n$ and $(BV\text{-}Q\text{-}BV^{6+})_n$, is a matter of degree. The quinone in NQ-BV^{3+} is slightly more reversible in acidic solution that the quinone in BV-Q-BV^{6+}.

Cyclic Voltammetry of Electrode-Confined $(NQ\text{-}BV\text{-}BV^{5+})_n$. The cyclic voltammogram shown in Figure 6 illustrates the 2:1 ratio of viologen to quinone in $(NQ\text{-}BV\text{-}BV^{5+})_n$. The overlapping waves at -0.40 V vs SCE represents the reduction of the quinone subunit and the first reduction of the two viologen subunits. The wave at -0.91 V vs SCE is the second reduction of the two viologen subunits ($BV^{+/0}$). The relative areas of the two waves are in accord with a $4e^-/2H^+$ reduction of NQ and $2BV^{2+}$ vs two $1e^-$ reductions ($1e^-/BV^{+\bullet}$) of $2BV^{+\bullet}$.

Electrodes (both glassy carbon and ITO) modified with high coverages of $(NQ\text{-}BV\text{-}BV^{5+})_n$ (data not shown) exhibit pH-

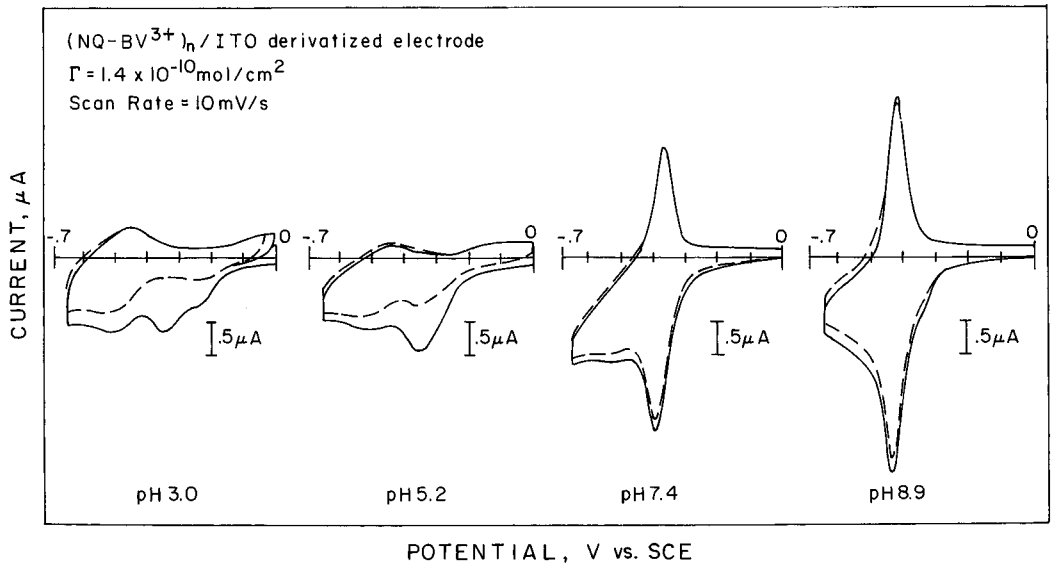

Figure 4. pH-dependent cyclic voltammograms of an ITO electrode derivatized with $(NQ\text{-}BV^{3+})_n$. The experimental conditions are the same as those described for Figure 2. Unlike a glassy carbon electrode with a similar coverage of **1a** (see Figure 3, part b), some trapping of charge occurs in a monolayer of **1a** confined to ITO.

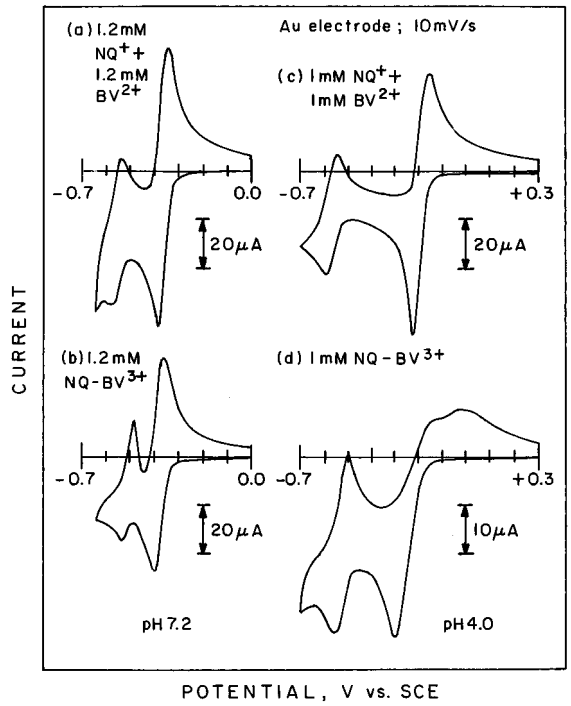

Figure 5. Comparison of the cyclic voltammograms of **1b** and a 1:1 mixture of **5b** and **9b** at neutral and acidic pH. At pH 7.2 (scans a and b), the electrochemistry of **1b** and the mixture is similar, whereas at pH 4 (scans c and d), the electrochemistry of the NQ subunit in **1b** is much less reversible than that of **5b** in the mixture.

dependent charge-trapping behavior similar to that of electrodes modified with $(NQ\text{-}BV^{3+})_n$ or $(BV\text{-}Q\text{-}BV^{6+})_n$. Glassy carbon electrodes modified with a monolayer of **2a**, however, do not trap charge at any pH (data not shown). Instead, a reversible, pH-dependent wave that shifts 59 mV per unit of pH is observed when changing from high to low pH, behavior that is observed when NQ subunits can exchange reducing equivalents directly with an electrode. The lack of charge trapping in monolayers of **2a** is somewhat surprising, considering that the link to the surface is via a −Si−O− bond at the terminal benzyl group. The flexibility of the molecules is, however, sufficient to allow the NQ/NQH_2 system to equilibrate directly with the surface of the electrode.

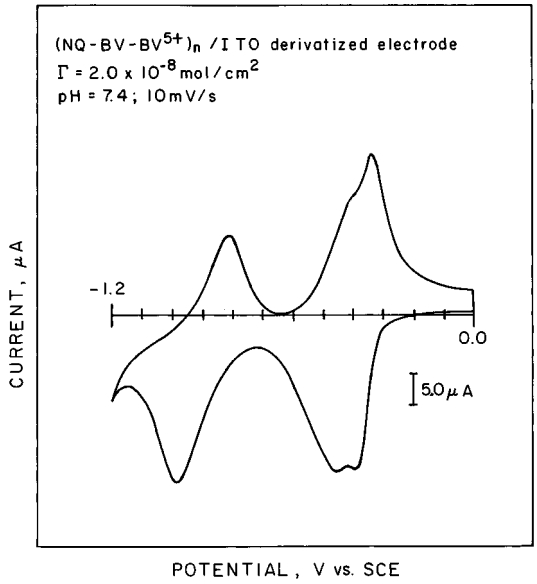

Figure 6. Cyclic voltammogram obtained in 1 M LiCl/pH 7.4 Tris buffer at 10 mV/s using an ITO electrode modified with $(NQ\text{-}BV\text{-}BV^{5+})_n$. Both the NQ/NQH_2 ($2e^-/2H^+$) and $BV^{2+/+\bullet}$ ($1e^-$) couples appear as overlapping reversible waves at −0.45 V. The $BV^{+\bullet/0}$ couple ($1e^-$) appears as a reversible wave at −0.91 V.

Cyclic Voltammetry of 2b. The cyclic voltammograms of **2b** at both pH 7.2 and 4.0 (data not shown) are comparable to those of an equimolar mixture of **5b** and 2 equiv of **9b** except for the presence of two stripping waves associated with the oxidation of precipitated $BV^{+\bullet}$. At much lower concentrations (μM) or faster scan rates (>200 mV/s), the stripping peaks disappear and separate waves for the oxidation of $BV^{+\bullet}$ and NQ/NQH_2 are observed. At pH 4.0, the wave for NQ/NQH_2 occurs at ∼−0.17 V vs SCE for both **2b** and **5b**. The electrochemical behavior of **2b** is different from that of **1b** (see Figure 5) at pH 4.0 in that the wave for the NQ/NQH_2 subunit in **2b** behaves exactly as observed for **5b** at this pH. This behavior is consistent with the results obtained from electrodes covalently modified with a monolayer of **2a**, where the electrochemistry of the NQ/NQH_2 couple is independent of the BV^{2+} subunit at all pHs.

Copolymerization of 1a or 2a with 1,2-Bis(trimethoxysilyl)ethane. Electrodes can be prepared with durable coverages

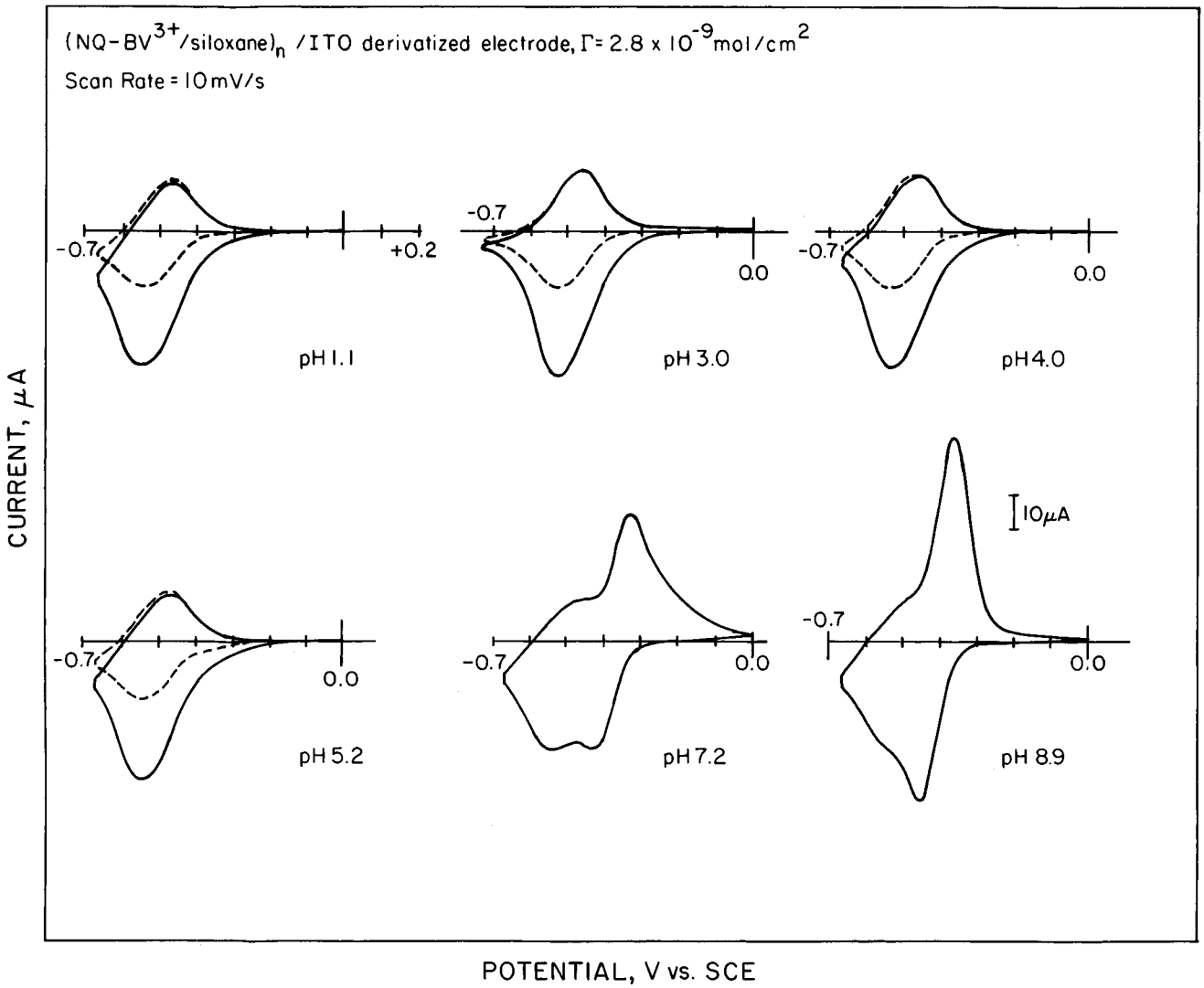

Figure 7. pH-dependent cyclic voltammograms of an ITO electrode derivatized with (NQ-BV^{3+}/siloxane)$_n$. The experimental conditions are the same as those described for Figure 2.

($>10^{-8}$ mol cm^{-2}) of (BV-Q-BV^{6+})$_n$ or (BV^{2+})$_n$. High coverages of (NQ-BV^{3+})$_n$ and (NQ-BV-BV^{5+})$_n$, however, are difficult to prepare and are often less durable than those of (BV-Q-BV^{6+})$_n$ or (BV^{2+})$_n$. The difficulty in maintaining high coverages of (NQ-BV^{3+})$_n$ and (NQ-BV-BV^{5+})$_n$ on electrode surfaces is probably due to the inability to form large cross-linked polymers with **1a** or **2a**. Further evidence of the inability to form large cross-linked polymers is that 1 mM solutions of **1a** or **2a** remain clear for days, while 1 mM solutions of **3** or **9a** turn cloudy after several hours. The relative difficulty in polymerizing **1a** or **2a** compared to that for **3** or **9a** is not unreasonable since **1a** and **2a** contain only one trimethoxysilyl group. Although there are three cross-linking points for each trimethoxysilyl moiety, the bulky NQ-BV^{3+} or NQ-BV-BV^{5+} unit may make multiple reactions at Si difficult. It seems likely that **1a** or **2a** form oligomers instead of polymers.

One way to increase the extent of polymerization of **1a** or **2a** is to make derivatives that have two trimethoxysilyl groups per monomer. Another, simpler method is to copolymerize **1a** or **2a** with a compound that contains two trimethoxysilyl groups. Accordingly, we examined the copolymerization of **1a** or **2a** with 1,2-bis(trimethoxysilyl)ethane. The resulting copolymers, abbreviated (NQ-BV^{3+}/siloxane)$_n$ or (NQ-BV-BV^{5+}/siloxane)$_n$, were prepared by mixing **1a** or **2a** with an equimolar amount of 1,2-bis(trimethoxysilyl)ethane in 0.2 M KCl/0.1 M K_2HPO_4. The derivatizing solutions of **1a** or **2a** turn cloudy 25−30 min after the addition of 1,2-bis(trimethoxysilyl)ethane, indicating fairly rapid polymerization. The most reproducible results were achieved by allowing the derivatization solution to "cure" for 15 min after the 1,2-bis(trimethoxysilyl)ethane was added and then cycling the electrode from −0.2 to −0.6 V vs SCE at 10 mV/s while the solution was stirred.[20] Coverages of (NQ-BV^{3+}/siloxane)$_n$ or (NQ-BV-BV^{5+}/siloxane)$_n$ of at least 1×10^{-8} mol cm^{-2} can be prepared in this fashion. Shown in Figure 7 are the cyclic voltammograms at different pHs of an electrode modified with (NQ-BV^{3+}/siloxane)$_n$. Similar behavior is observed for electrodes modified with (NQ-BV-BV^{5+}/siloxane)$_n$ (data not shown).

Cyclic voltammetry of electrodes modified with (NQ-BV^{3+}/siloxane)$_n$ or (NQ-BV-BV^{5+}/siloxane)$_n$ indicates the presence and relative amount of NQ and BV^{2+} in these copolymers, but not that of 1,2-bis(trimethoxysilyl)ethane. X-ray photoelectron spectroscopy (XPS) was used to determine the relative amount of 1,2-bis(trimethoxysilyl)ethane present in (NQ-BV^{3+}/siloxane)$_n$ and (NQ-BV-BV^{5+}/siloxane)$_n$. The ratio of Si:N was measured in the following samples: ITO/(NQ-BV^{3+})$_n$, ITO/(NQ-BV^{3+}/siloxane)$_n$, ITO/(NQ-BV-BV^{5+})$_n$, and ITO/(NQ-BV-BV^{5+}/siloxane)$_n$. The intensity of the Si signals was greater in the (NQ-BV^{3+}/siloxane)$_n$ and (NQ-BV-BV^{5+}/siloxane)$_n$ samples than in the (NQ-BV^{3+})$_n$ and (NQ-BV-BV^{5+})$_n$ samples. Shown in Figure 8, parts a and b, are typical survey spectra obtained from an ITO electrode modified with (NQ-BV^{3+})$_n$ and (NQ-

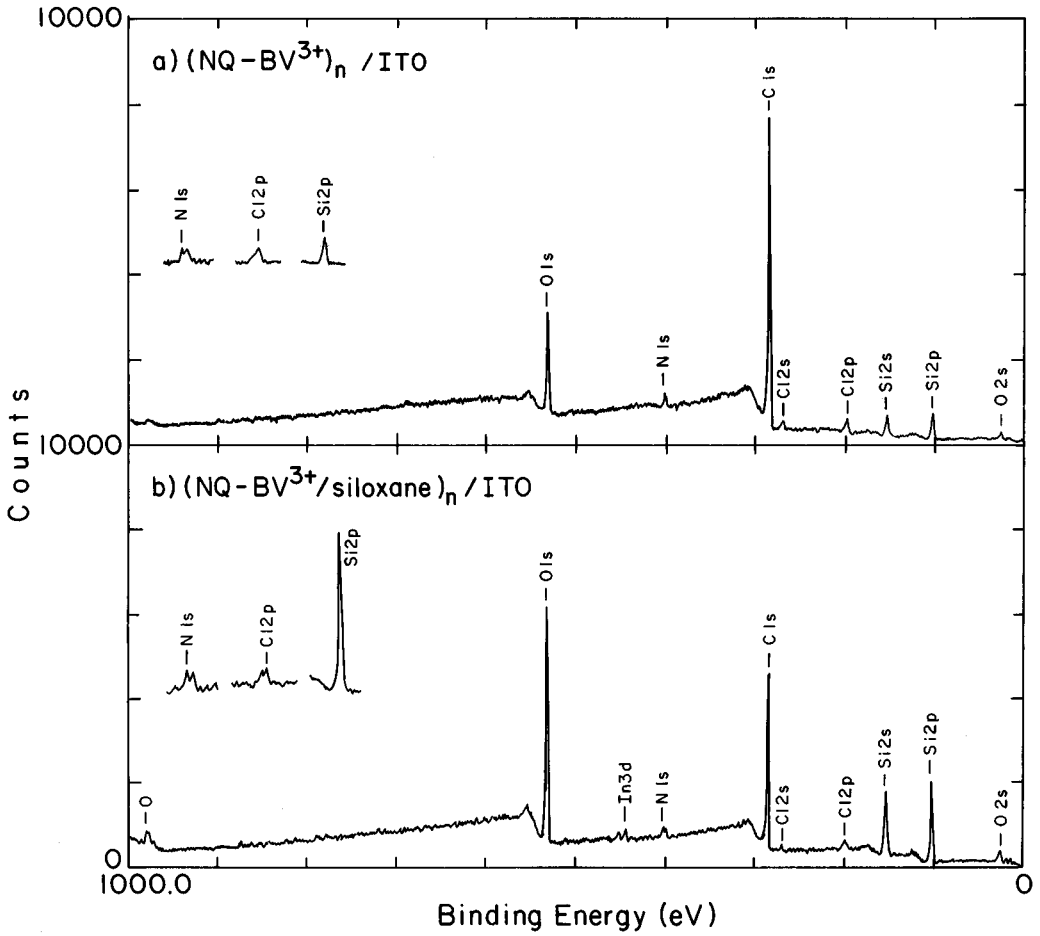

Figure 8. XPS survey spectra of (a) ITO/(NQ-BV^{3+})$_n$ and (b) ITO/(NQ-BV^{3+}/siloxane)$_n$. The insets are enlargements of the N(1s), Cl(2p), and Si(2p) signals. As expected, the Si signal is larger than the N signal in the ITO/(NQ-BV^{3+}/siloxane)$_n$ sample relative to the ITO/(NQ-BV^{3+})$_n$ sample. Analysis of the signal intensities indicates that there are ~1−2 equiv of 1,2-bis(trimethoxysilyl)ethane per equivalent of **1a** in the ITO/(NQ-BV^{3+}/siloxane)$_n$ sample.

BV^{3+}/siloxane)$_n$, respectively. Assuming the intensities of the Si(2p) and N(1s) signals in (NQ-BV^{3+})$_n$ correspond to a Si:N ratio of 0.25, we observed a relative ratio of 1.16:1 for the (NQ-BV^{3+}/siloxane)$_n$ sample, corresponding to a ratio of 1.81:1 1,2-bis(trimethoxysilyl)ethane:NQ-BV^{3+}.

To check the validity of the XPS measurement, the ratio of the Cl(2p) to N(1s) XPS signals was also examined in each sample. Although the electrodes were prepared and characterized in KCl solutions, the lack of a K signal in the XPS survey indicates that the observed Cl signals are due to covalent Cl in **1a** and **2a**. The ratio of the Cl(2p) to N(1s) signals should therefore be the same for both the ITO/(NQ-BV^{3+})$_n$ and ITO/(NQ-BV^{3+}/siloxane)$_n$ samples. The observed ratio for Cl(2p) to N(1s) is close: 1.0:1 for the ITO/(NQ-BV^{3+})$_n$ sample and 0.9:1 for the ITO/(NQ-BV^{3+}/siloxane)$_n$ sample. Similarly, ITO modified with (NQ-BV-BV^{5+})$_n$ or (NQ-BV-BV^{5+}/siloxane)$_n$ was examined by XPS (data not shown) and a ratio of 1.2:1 1,2-bis(trimethoxysilyl)ethane:NQ-BV-BV^{5+} was observed. The observed ratio for Cl(2p) to N(1s) for both the (NQ-BV-BV^{5+})$_n$ and (NQ-BV-BV^{5+}/siloxane)$_n$ samples are close: 0.7:1 for the (NQ-BV-BV^{5+})$_n$ sample and 0.6:1 for the (NQ-BV-BV^{5+}/siloxane)$_n$ sample.

Observation of Charge Trapping by Spectroelectrochemistry. Shown in Figure 9 are the absorption spectra of an ITO electrode modified with (NQ-BV-BV^{5+}/siloxane)$_n$ taken at different potentials. The spectra were recorded while the potential of the electrode was swept between 0.0 and −0.7 V vs SCE in acidic electrolyte. Initially, (NQ-BV-BV^{5+}/siloxane)$_n$ is fully oxidized at 0.0 V vs SCE, and the only absorbance in the visible region (460 nm) is due to the NQ chromophore. Upon sweeping the potential negative to −0.7 V at 10 mV/s, we found the absorption spectrum changes to reflect the reduction of both NQ and BV^{2+} subunits. The appearance of absorption bands at 372, 400, 555 and 605 nm indicates that both dimeric and monomeric forms of $BV^{+\bullet}$ are present in the reduced polymer. Returning the potential of the electrode to 0.0 V vs SCE, we found that the resulting absorption spectrum illustrates the trapping of charge in the form of NQH_2 at this pH (the absorption band for the NQ subunit at λ_{460} is absent). When the electrochemical cell is exposed to air, NQH_2 is slowly reoxidized to NQ, returning the absorption spectrum to its original state (the absorption band for the NQ subunit at λ_{460} reappears). The inset in Figure 9 (NQ/NQH_2 absorption band) illustrates the slow (typically ~30−40 min) reoxidation of NQH_2 to NQ by O_2. The ratio of absorbance at 460 nm at 0.0 V to the absorbance at 555 nm at −0.7 V confirms our assertion that the ratio of NQ:BV^{2+} in (NQ-BV-BV^{5+}/siloxane)$_n$ is 1:2, assuming $\epsilon_{soln} = \epsilon_{surf}$ for each of the chromophores.

Catalytic Release of Charge Trapped in (NQH_2-BV^{3+}/Siloxane)$_n$ and (NQH_2-BV-BV^{5+}/Siloxane)$_n$ with I_3^-/I^-. The redox couple I_3^-/I^- was used to access charge trapped in (NQH_2-BV^{3+}/siloxane)$_n$ and (NQH_2-BV-BV^{5+}/siloxane)$_n$ because it is soluble in aqueous acid and can diffuse through the polymer to deliver charge to the electrode. Scheme 4 illustrates the catalytic mechanism by which this mediation occurs. Oxidation of the NQH_2 centers occurs only when the potential of the electrode modified with (NQH_2-BV^{3+}/siloxane)$_n$ or (NQH_2-BV-BV^{5+}/siloxane)$_n$ is brought close to $E^{o\prime}(I_3^-/I^-)$ (0.45 V vs SCE). At

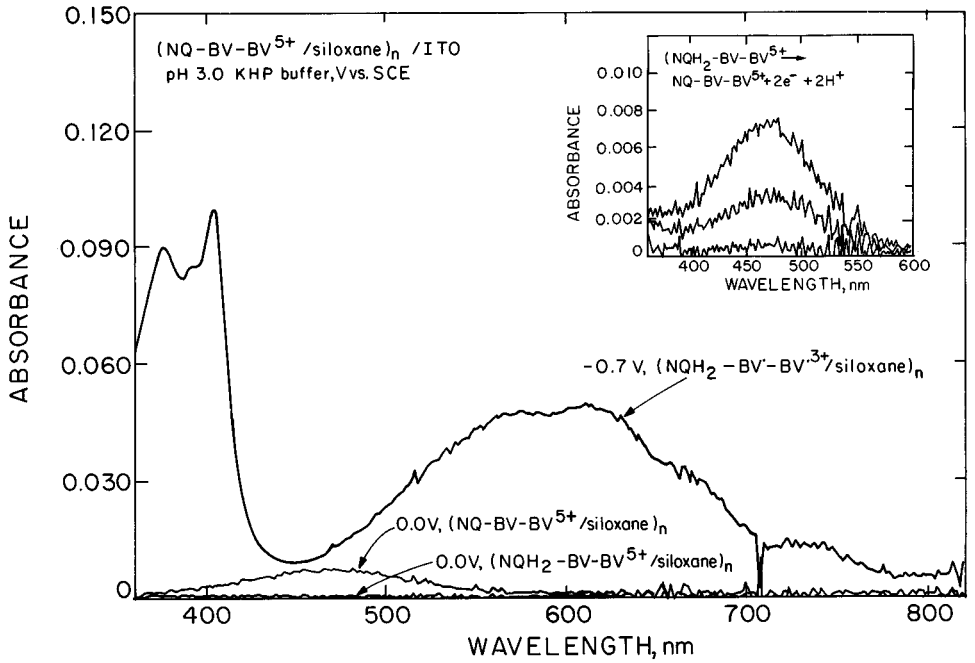

Figure 9. Spectroelectrochemical absorption spectra of an ITO electrode modified with (NQ-BV-BV^{5+}/siloxane)$_n$ ($\Gamma \approx 2 \times 10^{-9}$ mol cm^{-2}) at different potentials. The spectra were obtained while we swept the potential of the electrode between 0 and −0.7 V. The initial spectrum, obtained at 0.0 V, is of the fully oxidized polymer where the absorption at 460 nm is due to the NQ subunit. The spectrum obtained at −0.7 V vs SCE corresponds to the fully reduced polymer (NQH_2^+-$BV^{+\bullet}$-$BV^{+\bullet}$/siloxane)$_n$, where the absorbance maxima at 372, 400, 555, and 605 nm are due to the $BV^{+\bullet}$ subunits. Returning the potential to 0 V reveals the charge-trapping behavior of (NQ-BV-BV^{5+})$_n$/siloxane at pH 3.0. At this pH, the polymer remains partially reduced, (NQH_2^+-BV^{2+}-BV^{2+}/siloxane)$_n$, and the absorbance due to the NQ subunit at 460 nm is absent. The inset illustrates the slow (typically ∼30−40 min) reoxidation of NQH_2 to NQ by O_2.

SCHEME 4: Catalytic Release of Charge Trapped in the Form of NQH_2 in Homopolymers of 1 or 2 by Solutions Containing a Chemical Mediator, M

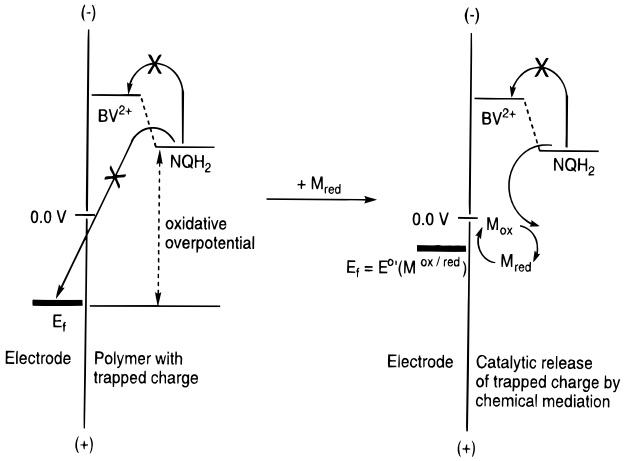

this potential, I_3^- is generated at the electrode surface and diffuses through the polymer, oxidizing NQH_2 to NQ and forming I^-. Charge is subsequently returned to the electrode by I^- where it is reoxidized to I_3^-, completing the catalytic cycle.

Figure 10 shows the cyclic voltammograms of a glassy carbon electrode modified with (NQ-BV^{3+}/siloxane)$_n$ obtained in the absence (Figure 10, part a) or presence (Figure 10, part b) of KI. The first and second scans in Figure 10, part a (represented as solid and dashed lines, respectively), show the reversible reduction of BV^{2+} subunits and the irreversible reduction of NQ subunits in (NQ-BV^{3+}/siloxane)$_n$. The difference between the integrated areas of the cathodic waves from the first and second scans accounts for the amount of charge trapped in the form of NQH_2. A potential excursion to +1.0 V vs SCE fails to oxidize most of the NQH_2 subunits, demonstrating that charge remains trapped even at high overpotentials. Note that $E^{o\prime}$(NQ/NQH_2) at this pH is ∼−0.15 V, as indicated by the small prewave at this potential. The third cycle in Figure 10, part a (represented as a dotted line), shows that ∼30% of the NQH_2 subunits in (NQH_2-BV^{3+}/siloxane)$_n$ for this particular electrode were oxidized by the potential excursion to +1.0 V.

Shown in Figure 10, part b, is the cyclic voltammetry of the same electrode in 0.5 M KCl/pH 3.0 phosphate buffer containing a catalytic amount of KI (150 μM). The first and second cycles between +0.15 and −0.65 V show that KI does not disturb the charge-trapping behavior of an electrode modified with (NQ-BV^{3+}/siloxane)$_n$. A potential excursion to +1.0 V (dashed line), however, results in the mediated release of trapped charge. When the electrode potential is near $E^{o\prime}(I_3^-/I^-)$, enough I_3^- is produced (eq 1) to catalytically oxidize NQH_2 to NQ (oxidative wave at +0.85 V). The I^- generated from this reaction subsequently delivers charge to the electrode and becomes reoxidized to I_3^- to complete the catalytic cycle (eq 2). The third cycle (represented as a dotted line) shows the underlying I_3^-/I^- electrochemistry at ∼0.45 V. The difference in shape and the large peak to peak separation between the cathodic and anodic waves of the I_3^-/I^- couple reflects a difference in mobility of I_3^- and I^- in this highly cross-linked polymer. A glassy carbon electrode modified with (BV-Q-BV^{6+})$_n$ shows a symmetrically shaped cyclic voltammogram for the I_3^-/I^- couple with a peak to peak separation of 60 mV under equivalent conditions.[3]

$$NQH_2 + I_3^- \rightarrow NQ + 2H^+ + 3I^- \quad (1)$$

$$3I^- \rightarrow I_3^- + 2e^- \quad (2)$$

The electrochemical behavior of an electrode modified with (NQ-BV-BV^{5+}/siloxane)$_n$ is essentially equivalent to that of an electrode modified with (NQ-BV^{3+}/siloxane)$_n$ under the conditions described above [i.e., charge trapped as NQH_2 is catalytically released in the presence of I_3^-/I^- when the potential of the electrode is near $E^{o\prime}(I_3^-/I^-)$]. The only exception is the percentage of charge trapped in the different polymers. For

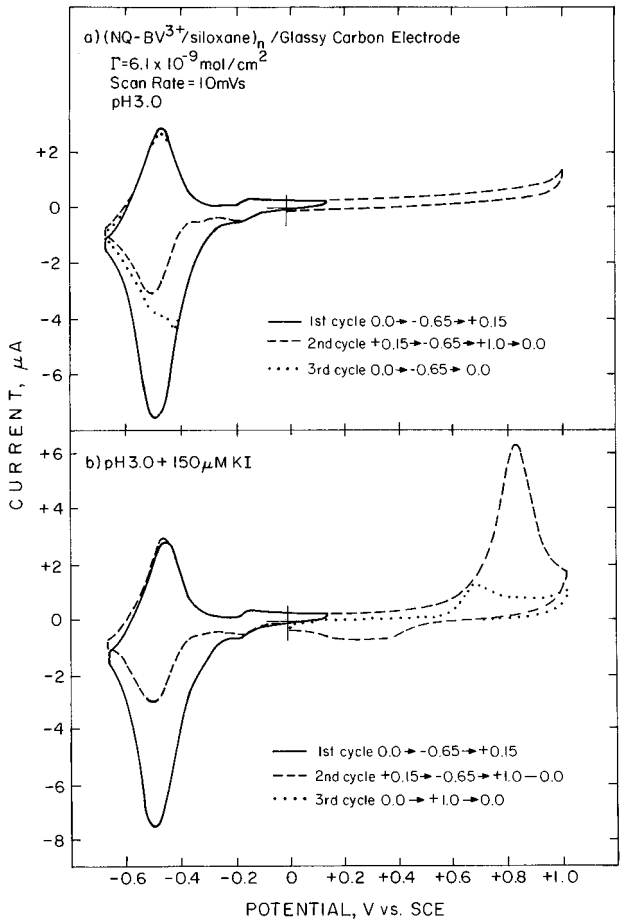

Figure 10. Cyclic voltammograms obtained in the absence (Figure 10, part a) or presence (Figure 10, part b) of KI in 0.5 M KCl/pH 3.0 phosphate buffer using a glassy carbon electrode derivatized with $(NQ\text{-}BV^{3+}/siloxane)_n$: (a) 0.5 M KCl/pH 3.0 phosphate buffer; (b) 150 μM KI/0.5 M KCl/pH 3.0 phosphate buffer. The potential of the electrode was scanned as indicated in the figure. The potential excursion to +1.0 V vs SCE in part a fails to oxidize most of the NQH_2 subunits, demonstrating that charge remains trapped even at high overpotentials. Note that $E^{o\prime}(NQ/NQH_2)$ at this pH is $\sim$−0.15 V as seen by the small prewave at this potential. In the presence of KI (b), a potential excursion to +1.0 V, however, results in the mediated release of trapped charge because enough I_3^- is produced to catalytically oxidize NQH_2 to NQ.

$(NQ\text{-}BV^{3+}/siloxane)_n$, the ratio of NQ to BV^{2+} is 1:1; therefore, 67% of the charge injected into the polymer remains trapped at acidic pH. The ratio of NQ to BV^{2+} in $(NQ\text{-}BV\text{-}BV^{5+}/siloxane)_n$, however, is 1:2, and therefore only 50% of the charge injected into $(NQ\text{-}BV\text{-}BV^{5+}/siloxane)_n$ remains trapped. Consequently, the electrochemical wave that results from the catalytic oxidation of NQH_2 by I_3^- is smaller for electrodes modified with $(NQ\text{-}BV\text{-}BV^{5+}/siloxane)_n$ than those modified with $(NQ\text{-}BV^{3+}/siloxane)_n$.

Electrodes Modified with $(NQ\text{-}BV^{3+}/Siloxane)_n$ or $(NQ\text{-}BV\text{-}BV^{5+}/Siloxane)_n$ Do Not Electrostatically Bind $Fe(CN)_6^{3-/4-}$. Our attempts to utilize the $Fe(CN)_6^{3-/4-}$ couple as a catalytic mediator to release charge trapped in $(NQH_2\text{-}BV^{3+}/siloxane)_n$ and $(NQH_2\text{-}BV\text{-}BV^{5+}/siloxane)_n$ were unsuccessful. Different from the I_3^-/I^- couple, the anionic redox couple $Fe(CN)_6^{3-/4-}$ is known to electrostatically concentrate into polycationic polymers.[3,15,21−25] Electrodes modified with $\sim 10^{-9}$ mol cm^{-2} of either $(NQ\text{-}BV^{3+}/siloxane)_n$ or $(NQ\text{-}BV\text{-}BV^{5+}/siloxane)_n$, however, show little or no electrostatic binding of $Fe(CN)_6^{3-/4-}$.

Figure 11 shows the results obtained when an electrode modified with $(NQ\text{-}BV\text{-}BV^{5+}/siloxane)_n$ is cycled in 0.1 M KCl/

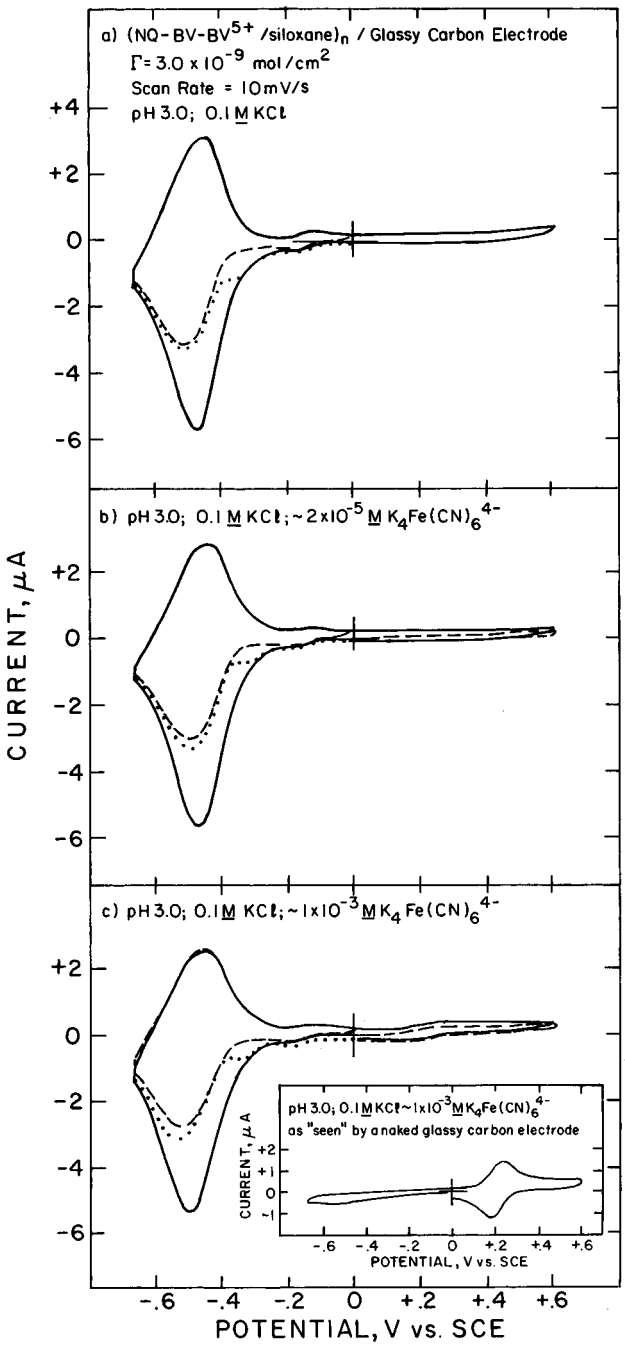

Figure 11. Cyclic voltammograms obtained with and without $K_4Fe(CN)_6$ dissolved in the electrolyte using a glassy carbon electrode derivatized with $(NQ\text{-}BV\text{-}BV^{5+}/siloxane)_n$: (a) 0.1 M KCl/pH 3.0 buffer only; (b) $\sim 2 \times 10^{-5}$ M $K_4Fe(CN)_6$ added to electrolyte; (c) $\sim 1 \times 10^{-3}$ M $K_4Fe(CN)_6$ added to electrolyte. The inset in part c is the cyclic voltammogram obtained in $\sim 1 \times 10^{-3}$ M $K_4Fe(CN)_6$/0.1 M KCl/pH 3.0 buffer using a clean carbon electrode equivalent in size to the modified carbon electrode.

pH 3.0 buffer with or without $K_4Fe(CN)_6$ present. An electrode modified with $(NQ\text{-}BV^{3+}/siloxane)_n$ shows similar behavior under the same conditions (data not shown). Each cyclic voltammogram, except the inset in part c, comprises three cycles where the potential is scanned as follows: 0.0 → −0.65 → 0.0 V vs SCE in the first cycle (solid line), 0.0 → −0.65 → +0.6 → 0.0 V vs SCE in the second cycle (dashed line), and 0.0 → +0.6 → −0.65 → 0.0 V vs SCE in the third cycle (dotted line). The cathodic wave in the first cycle represents the total amount of charged injected into the polymer. The difference in the integrated areas between the cathodic waves of the first and

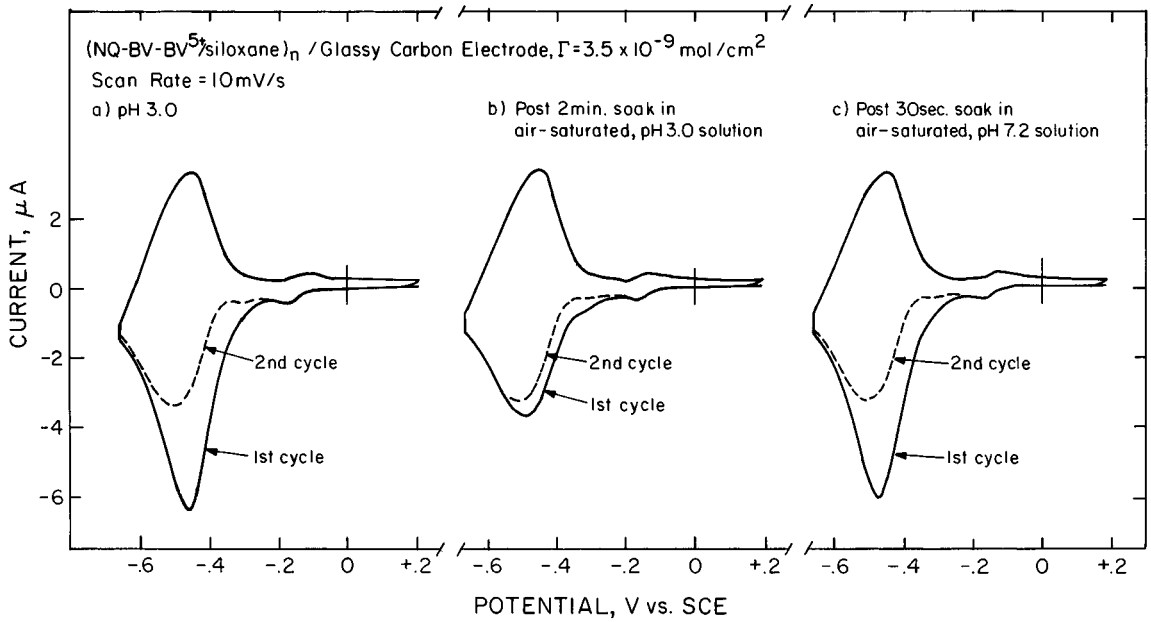

Figure 12. Demonstration of the oxidation of NQH_2 in $(NQH_2\text{-BV-BV}^{5+}/\text{siloxane})_n$ by O_2 at a glassy carbon electrode modified with $(\text{NQ-BV-BV}^{5+}/\text{siloxane})_n$. All cyclic voltammograms were obtained by cycling the potential of the electrode between +0.2 and −0.65 V vs SCE in 0.5 M KCl/pH 3.0 buffer purged with Ar. The initial cyclic voltammograms shown in part a exhibit typical charge-trapping behavior of an electrode modified with $(NQH_2\text{-BV-BV}^{5+}/\text{siloxane})_n$ at pH 3.0. Shown in part b are the cyclic voltammograms obtained after dipping the electrode for 2 min in 0.5 M KCl/pH 3.0 phosphate buffer saturated with air. The cyclic voltammogram shown in part c was obtained after dipping the electrode for 30 s in 0.5 M KCl/pH 7.2 Tris buffer solution saturated with air. The results obtained at acidic pH (b) compared to those at neutral pH (c) clearly indicate that the kinetics for the oxidation of NQH_2 by O_2 are pH-dependent.

second cycles (negative to 0.0 V) represents the amount of charge trapped as NQH_2.

Similar to what was observed with an electrode modified with $(\text{NQ-BV}^{3+}/\text{siloxane})_n$ (Figure 10, part a), charge is not released from $(NQH_2\text{-BV-BV}^{5+}/\text{siloxane})_n$ even at large oxidizing overpotentials (Figure 11, part a). The cyclic voltammogram obtained when 2×10^{-5} M $K_4Fe(CN)_6$ is added to the electrolyte (Figure 11, part b) is essentially identical to that obtained in Figure 11, part a. For this particular electrode, no electrochemical signal is observed for the $Fe(CN)_6^{3-/4-}$ couple at +0.2 V vs SCE. Earlier work using the $Fe(CN)_6^{3-/4-}$ couple as a catalytic mediator for the release of charge from $(\text{BV-QH}_2\text{-BV}^{6+})_n$ demonstrated that $\sim 0.1n$ mol of $Fe(CN)_6^{3-/4-}$ incorporated into the polymer was capable of oxidizing all of the hydroquinone subunits in $(\text{BV-QH}_2\text{-BV}^{6+})_n$.[3] We assert that the permeability of $(\text{NQ-BV-BV}^{5+}/\text{siloxane})_n$, as well as $(\text{NQ-BV}^{3+}/\text{siloxane})_n$, to $Fe(CN)_6^{3-/4-}$ is compromised by the added cross-linking provided by the siloxane copolymerizing reagent 1,2-bis(trimethoxysilyl)ethane. A quick way to check the validity of this assertion is to immerse the electrode into a more concentrated solution of $K_4Fe(CN)_6$. Figure 11, part c, shows the cyclic voltammogram obtained when the concentration of $K_4Fe(CN)_6$ in the electrolyte is $\sim 1 \times 10^{-3}$ M. The small wave at +0.2 V vs SCE in Figure 11, part c, is due to the $Fe(CN)_6^{3-/4-}$ couple but represents only a small fraction of the $Fe(CN)_6^{3-/4-}$ actually present and is probably due to pinholes in the polymer. The inset is the cyclic voltammogram of the same solution using a clean carbon electrode of similar size (note the different current scale). Unlike other cationic polymers, electrodes modified with $(\text{NQ-BV}^{3+}/\text{siloxane})_n$ and $(\text{NQ-BV-BV}^{5+}/\text{siloxane})_n$ do not electrostatically concentrate $Fe(CN)_6^{3-/4-}$ and, consequently, the $Fe(CN)_6^{3-/4-}$ couple is ineffective in mediating the release of trapped charge in either of these polymers.

Oxidation of NQH_2 in $(NQH_2\text{-BV}^{3+}/\text{Siloxane})_n$ or $(NQH_2\text{-BV-BV}^{5+}/\text{Siloxane})_n$ by O_2. Earlier work demonstrated the oxidation of NQH_2 to NQ by O_2 both in solution and surface-confined naphthoquinones and the consequential formation of H_2O_2 product (eq 3).[15,16] Shown in Figure 12 are the results

$$NQH_2 + O_2 \rightarrow NQ + H_2O_2 \qquad (3)$$

from an experiment that demonstrates the oxidation of NQH_2 in $(NQH_2\text{-BV-BV}^{5+}/\text{siloxane})_n$ by O_2. A glassy carbon electrode modified with $(\text{NQ-BV-BV}^{5+}/\text{siloxane})_n$ was suspended in deoxygenated 0.5 M KCl/pH 3.0 buffer and cycled between +0.2 and −0.65 V vs SCE to produce the $(NQH_2\text{-BV-BV}^{5+}/\text{siloxane})_n$ state (Figure 12, part a). The electrode was subsequently transferred to an equivalent electrolyte saturated with air and soaked for 2 min. The electrode was then returned to the original deoxygenated electrolyte (0.5 M KCl/pH 3.0 buffer) and cycled between +0.2 and −0.65 V vs SCE (Figure 12, part b). Essentially no NQH_2 was oxidized by the O_2 dissolved in the acidic electrolyte since the first and second cycle in Figure 12, part b, are nearly identical to the second cycle in Figure 12, part a. When the electrode is quickly dipped into an air-saturated electrolyte comprised of 0.5 M KCl/pH 7.2 Tris buffer, the subsequent cyclic voltammogram indicates that all of the NQH_2 subunits were reoxidized (Figure 12, part c). To confirm that O_2 in the air-saturated 0.5 M KCl/pH 7.2 Tris buffer solution was responsible for the oxidation of the NQH_2 subunits, the electrode was transferred under a stream of argon to a deoxygenated electrolyte of equivalent composition (0.5 M KCl/pH 7.2 Tris buffer) for ~30 s, whereupon the subsequent cyclic voltammogram in 0.5 M KCl/pH 3.0 phosphate buffer solution was identical to that in Figure 12, part b.

The results from an identical experiment (*vide supra*) using a glassy carbon electrode modified with $(\text{NQ-BV}^{3+}/\text{siloxane})_n$ are similar except for differences that reflect the ratio of NQ:BV^{2+} (data not shown). Similar to what we found with $(\text{BV-Q-BV}^{6+})_n$, the rate at which O_2 oxidizes NQH_2 is pH-dependent.[3] Regardless of the kinetic limitations to O_2 reduction at acidic pH,[26] oxidation of NQH_2 by O_2 irreversibly produces H_2O_2, precluding delivery of released charge to the electrode. It should be noted that the time needed for the oxidation of

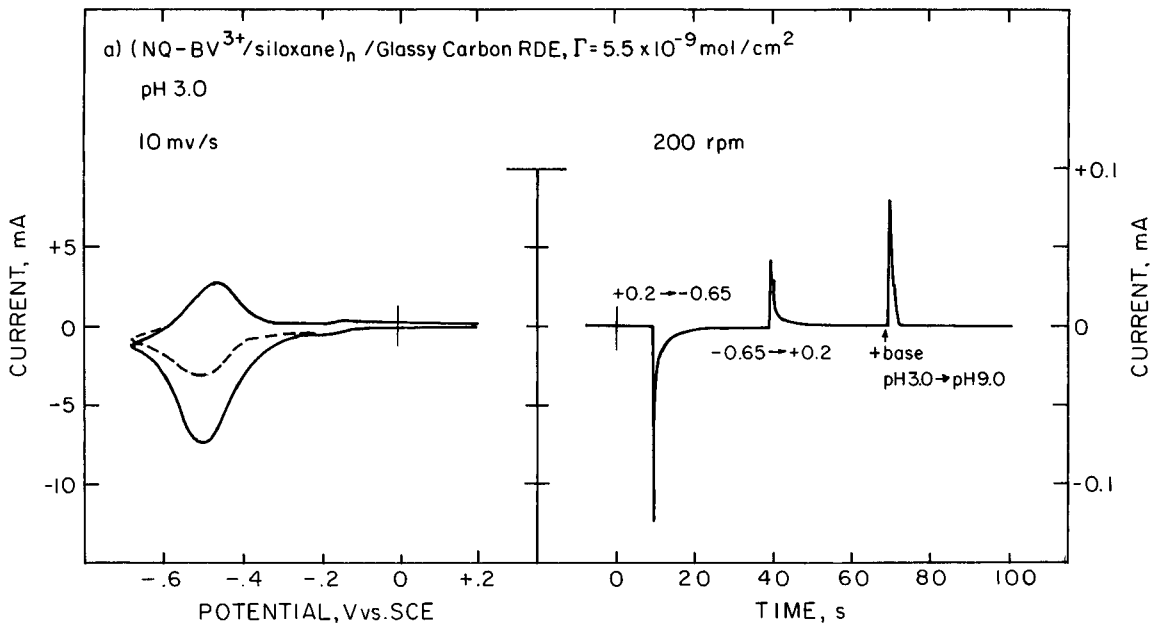

Figure 13. Demonstration of charge release from a glassy carbon RDE modified with $(NQ\text{-}BV^{3+}/siloxane)_n$ by a rapid increase in pH. The cyclic voltammogram shows typical charge-trapping behavior for this electrode in 0.5 M KCl/pH 3.0 phosphate buffer. The current−time profile illustrates how a rapid increase in pH releases charge trapped in $(NQH_2\text{-}BV^{3+}/siloxane)_n$. At $t = 0$ s, the potential of the electrode is +0.2 V vs SCE, and the polymer is in the fully oxidized state, $(NQ\text{-}BV^{3+}/siloxane)_n$. A potential step to −0.65 V fully reduces the polymer, resulting in a cathodic current at $t = 10$ s equivalent to $1ne^-$ per BV^{2+} subunit and $2ne^-$, $2H^+$ per NQ subunit. Stepping the potential back to +0.2 V produces the charge-trapped state $(NQH_2\text{-}BV^{3+}/siloxane)_n$, resulting in an anodic current at $t = 40$ s equivalent to $1ne^-$'s per BV^{2+} subunit. Injection of base at $t = 70$ s increases the pH so that the charge trapped as NQH_2 is released. The relative integrated area of the currents observed at 10, 40, and 70 s are 1, 0.33, and 0.67, respectively.

SCHEME 5: pH Jump Experiment Where Addition of Base to the Electrolyte Solution Causes an Increase in pH and a Shift in $E^{\circ\prime}$(NQ/NQH$_2$) Whereby the Energetics Are Such That the BV^{2+} Subunit Can Mediate the Reoxidation of NQH_2

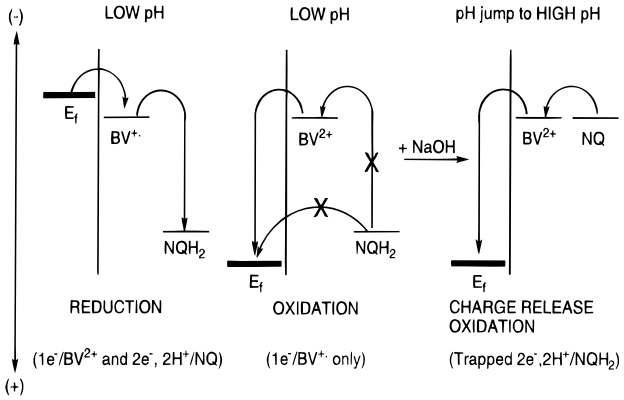

NQH_2 by O_2 at neutral pH varies from electrode to electrode; thus, quantification of this rate proves difficult.

pH Jump Experiments. Charge trapped in $(NQH_2\text{-}BV^{3+}/siloxane)_n$ or $(NQH_2\text{-}BV\text{-}BV^{5+}/siloxane)_n$ can be released by raising the pH of the electrolyte above neutral. The thermodynamic mechanism by which this occurs is illustrated in Scheme 5. An increase in pH shifts the pH-dependent $E^{\circ\prime}$(NQ/NQH_2) to a potential where BV^{2+} can mediate the reoxidation of NQH_2 and deliver the released charge to the electrode. Shown in Figure 13 are the cyclic voltammogram (0.5 M KCl/pH 3.0 phosphate buffer, 10 mV/s) and the current−time profile (200 rpm) of a glassy carbon RDEs modified with $(NQ\text{-}BV^{5+}/siloxane)_n$. The cyclic voltammogram demonstrates typical charge-trapping behavior, and the current−time profile illustrates the release of charge trapped in $(NQH_2\text{-}BV^{3+}/siloxane)_n$ as a consequence of a jump in pH.

An electrode modified with $(NQ\text{-}BV^{3+}/siloxane)_n$ or $(NQ\text{-}BV\text{-}BV^{5+}/siloxane)_n$ (data not shown) is initially held at +0.2 V vs SCE (0.5 M KCl/pH 3.0 phosphate buffer) to ensure full oxidation of the polymers. The potential is then stepped to −0.65 V vs SCE, where $1ne^-$ per BV^{2+} subunit and $2ne^-$, $2nH^+$ per NQ subunit are injected into the polymers. The injection of charge into $(NQ\text{-}BV^{3+}/siloxane)_n$ occurs as a transient cathodic current at $t = 10$ s in the current−time profile shown in Figure 13. The potential is subsequently stepped back to +0.2 V vs SCE to generate a transient anodic current at $t = 40$ s that corresponds to the partial oxidation of polymer to a charge-trapped state. In Figure 13, the integrated area of the anodic current at $t = 40$ s is one-third that of the cathodic current at $t = 10$ s and, thus, represents the oxidation of only the $BV^{+\bullet}$ subunits but not the NQH_2 subunits in $(NQH_2^+\text{-}BV^{+\bullet}/siloxane)_n$. Injection of ∼1 mL of 1 M NaOH into the electrochemical cell increases the pH to >9 and results in a second transient anodic current at $t = 70$ s (twice the integrated area of the anodic current at $t = 40$ s), corresponding to the release of charge trapped as NQH_2. The 1:2 ratio of the transient anodic currents ($t = 40$ s:$t = 70$ s) in Figure 13 illustrates the ratio of BV^{2+} subunits to NQ subunits in $(NQ\text{-}BV^{3+}/siloxane)_n$. By increasing the pH of the surrounding electrolyte, was found that the BV^{2+} subunits can mediate the release of charge from $(NQH_2\text{-}BV^{3+}/siloxane)_n$ and deliver it to the electrode.

Conclusions

The objective of this work was to determine the generality of pH-dependent rectification in quinone−viologen polymers. Electrodes modified with $(NQ\text{-}BV^{3+})_n$ or $(NQ\text{-}BV\text{-}BV^{5+})_n$, derived from **1a** or **2a**, respectively, show electrochemical behavior similar to that of the previously examined $(BV\text{-}Q\text{-}BV^{6+})_n$. Athough charge in the form of reduced quinone NQH_2 is trapped in both $(NQ\text{-}BV^{3+})_n$ and $(NQ\text{-}BV\text{-}BV^{5+})_n$ at low pH, surfaces modified with $(NQ\text{-}BV^{3+})_n$ and $(NQ\text{-}BV\text{-}BV^{5+})_n$ typically exhibit some degree of direct quinone electrochemistry,

as evidenced by a NQ/NQH_2 wave at low pH. Direct quinone electrochemistry is not observed at surfaces modified with $(BV\text{-}Q\text{-}BV^{6+})_n$. Additionally, a carbon electrode modified with monolayers of **2a** exhibits reversible quinone electrochemistry at all pHs. We attribute this result to the inherent flexibility of **2a** and the known adsorption properties of quinones on carbon. In contrast to results for monolayers of **1a** and **2a** on carbon, monolayers of **1a** and **2a** confined to ITO exhibit a decrease in the amount of directly accessible NQ/NQH_2 and, consequently, show some degree of charge trapping.

Electrodes modified with durable, thick coatings of $(NQ\text{-}BV^{3+})_n$ and $(NQ\text{-}BV\text{-}BV^{5+})_n$ are difficult to prepare. This difficulty, relative to the situation for $(BV^{2+})_n$ or $(BV\text{-}Q\text{-}BV^{6+})_n$, is due to **1a** or **2a** having only one $-Si(OMe)_3$ group. The technique of copolymerizing **1a** or **2a** with 1,2-bis(trimethoxysilyl)ethane is, therefore, a simple method to increase the thickness and durability of electrode-confined siloxane polymers derived from monomers that contain only one $-Si(OMe)_3$ group.

Several methods for the release of charge trapped in $(NQH_2\text{-}BV^{3+}/\text{siloxane})_n$ and $(NQH_2\text{-}BV\text{-}BV^{5+}/\text{siloxane})_n$ at low pH are demonstrated. The redox couple I_3^-/I^- releases trapped charge by a catalytic mechanism when the electrode potential is such that a small amount of I_3^- is generated, which, in turn, can oxidize NQH_2. Surprisingly, both $(NQ\text{-}BV^{3+}/\text{siloxane})_n$- and $(NQ\text{-}BV\text{-}BV^{5+}/\text{siloxane})_n$-modified electrodes are essentially impermeable to the larger redox couple $Fe(CN)_6^{3-/4-}$ and do not exhibit the "concentrating effect" of this anion as found with other cationic polymers. As a consequence, catalytic release of charge trapped in $(NQH_2\text{-}BV^{3+}/\text{siloxane})_n$ and $(NQH_2\text{-}BV\text{-}BV^{5+}/\text{siloxane})_n$ by $Fe(CN)_6^{3-/4-}$ is not observed. Oxidation of NQH_2 by O_2 occurs rapidly at neutral, but not acidic pH. The pH jump experiments illustrate how a rapid increase in pH can induce the release of trapped charge by shifting the pH-dependent $E°'(NQ/NQH_2)$ to a potential where the NQH_2 and BV^{2+} subunits equilibrate and allow the reoxidation of the NQH_2 to NQ with charge subsequently returned to the electrode.

We conclude that pH-dependent charge trapping in $(NQ\text{-}BV^{3+})_n$ and $(NQ\text{-}BV\text{-}BV^{5+})_n$ indicates that these polymers behave as if they were bilayer assemblies consisting of an inner layer (nearest the electrode) of $(BV^{2+})_n$ and an outer layer (nearest the electrolyte solution) of $(NQ)_n$, similar to the bilayer assemblies previously reported.[7,11] Unlike bilayer assemblies consisting of $(BV^{2+})_n$ and $(Q)_n$ units, however, where the slow rate of self-exchange between quinones prevents electrochemical communication with quinones not in direct contact with the $(BV^{2+})_n$ inner layer,[2] electrochemical communication with NQ units occurs throughout $(NQ\text{-}BV^{3+})_n$ and $(NQ\text{-}BV\text{-}BV^{5+})_n$, thus their behavior as "homogeneous bilayers". The significant implication of a homogeneous bilayer is that more NQ units are accessible relative to the amount accessible in a conventional bilayer; thus, a larger amount of charge can be trapped in $(NQ\text{-}BV^{3+})_n$ and $(NQ\text{-}BV\text{-}BV^{5+})_n$ polymers relative to the amount trapped in a conventional bilayer assembly of $(BV^{2+})_n$ and $(Q)_n$ units.

Acknowledgment. We gratefully acknowledge the U.S. Department of Energy, Office of Basic Energy Sciences, Division of Chemical Sciences, for generous support of this research. We acknowledge use of the XPS facility acquired through the joint Harvard/MIT University Research Initiative funded by the Defense Advanced Research Projects Agency.

References and Notes

(1) Smith, D. K.; Lane, G. A.; Wrighton, M. S. *J. Am. Chem. Soc.* **1986**, *108*, 3522.

(2) Smith, D. K.; Lane, G. A.; Wrighton, M. S. *J. Phys. Chem.* **1988**, *92*, 2616.

(3) Smith, D. K.; Tender, L. M.; Lane, G. A.; Licht, S.; Wrighton, M. S. *J. Am. Chem. Soc.* **1989**, *111*, 1099.

(4) Hable, C. T.; Crooks, R. M.; Wrighton, M. S. *J. Phys. Chem.* **1989**, *93*, 1190.

(5) Wrighton, M. S.; Palmore, G. T. R.; Hable, C. T.; Crooks, R. M. Multi-Component Redox Materials for Charge-Trapping: pH-Dependent 'Rectification' Using Viologen/Quinone Systems. In *New Aspects of Organic Chemistry*; Yoshida, Z., Shiba, T., Ohshiro, Y., Eds. VCH Publishers: New York, 1989; p 277.

(6) Hable, C. T.; Valentine, J. R.; Giasson, R.; Wrighton, M. S. *J. Phys. Chem.* **1993**, *97*, 6060.

(7) Abruña, H. D.; Denisevich, P.; Umana, M.; Meyer, T. J.; Murray, R. W. *J. Am. Chem. Soc.* **1981**, *103*, 1.

(8) Hillman, A. R.; Mallen, E. F. *J. Electroanal. Chem.* **1990**, *281*, 109.

(9) Li, Z.; Wand, C. M.; Persaud, L.; Mallouk, T. E. *J. Phys. Chem.* **1988**, *92*, 2592.

(10) Chidsey, C. E. D.; Murray, R. W. *Science* **1986**, *231*, 25.

(11) Vining, W. J.; Surridge, N. A.; Meyer, T. J. *J. Phys. Chem.* **1986**, *90*, 2281.

(12) Leidner, C. R.; Murray, R. W. *J. Am. Chem. Soc.* **1985**, *107*, 551.

(13) Pickup, P. G.; Kutner, W.; Leidner, C. R.; Murray, R. W. *J. Am. Chem. Soc.* **1984**, *106*, 1991.

(14) Denisevich, P.; William, K. W.; Murray, R. W. *J. Am. Chem. Soc.* **1981**, *103*, 4727.

(15) Calabrese, G. S.; Buchanan, R. M.; Wrighton, M. S. *J. Am. Chem. Soc.* **1983**, *105*, 5594.

(16) Calabrese, G. S.; Buchanan, R. M.; Wrighton, M. S. *J. Am. Chem. Soc.* **1982**, *104*, 786.

(17) Cheng, R. K. Y. Z.; Podrebarac, E. G.; Menon, C. S.; Cheng, C. *J. Med. Chem.* **1979**, *22*, 501.

(18) Brown, A. P.; Koval, C.; Anson, F. C. *J. Electroanal. Chem.* **1976**, *72*, 379.

(19) Soriaga, M. P.; Hubbard, A. T. *J. Am. Chem. Soc.* **1982**, *104*, 2735, 2742, 3937.

(20) Cycling the electrode during derivatization was necessary in order to monitor the growth of the surface-confined material. If the electrode is just held at reducing potentials, it is difficult to achieve reproducible results because the time required to achieve a given coverage depends on the lifetime of the solution. It was also necessary to stir the solution because, without stirring, the surface-confined wave stops growing after a short time. Presumably this is due to the decreasing diffusion coefficient of the growing $(NQ\text{-}BV^{3+}/\text{siloxane})_n$ or $(NQ\text{-}BV\text{-}BV^{5+}/\text{siloxane})_n$ particles in solution.

(21) Dominey, R. N.; Lewis, T. J.; Wrighton, M. S. *J. Phys. Chem.* **1983**, *87*, 5345.

(22) Simon, R. A.; Mallouk, T. E.; Daube, K. A.; Wrighton, M. S. *Inorg. Chem.* **1985**, *24*, 3119.

(23) Bruce, J. A.; Wrighton, M. S. *J. Am. Chem. Soc.* **1982**, *104*, 74.

(24) Sumi, K.; Anson, F. C. *J. Phys. Chem.* **1986**, *90*, 3845.

(25) Oyama, N.; Anson, F. C. *J. Electrochem. Soc.* **1980**, *127*, 247.

(26) Nagaoka, T.; Sakai, T.; Ogura, K.; Yoshino, T. *Anal. Chem.* **1986**, *58*, 1953.